Geomorphology 371 (2020) 107430

Contents lists available at ScienceDirect

Geomorphology

journal homepage: www.elsevier.com/locate/geomorph

Provenance in drainage integration research: Case studies from the Phoenix metropolitan area, south-central Arizona

Ronald I. Dorn [a,*], Steve J. Skotnicki [b], A. Wittmann [c], M. Van Soest [d]

[a] School of Geographical Sciences & Urban Planning, Arizona State University, Tempe, AZ 85287, USA
[b] 281 W. Amoroso Dr., Gilbert, AZ 85233, USA
[c] John M. Cowley Center for High Resolution Electron Microscopy, Eyring Materials Center, Arizona State University, Tempe, AZ 85287, USA
[d] School of Earth and Space Exploration, Arizona State University, Tempe 85287, USA

ARTICLE INFO

Article history:
Received 3 September 2018
Received in revised form 12 September 2020
Accepted 13 September 2020
Available online 16 September 2020

Keywords:
Basalt
Basin and Range Province
Drainage integration
Extensional tectonic terrain
Salt River

ABSTRACT

Studies of the evolution of drainage systems in extensional settings like the Basin and Range Province of western North America benefit from well drilling as a means of acquiring valuable insight. Cuttings from two wells drilled into sediments of the Phoenix metropolitan region, Arizona, USA, offer new insights into the drainage history of the Salt and Verde river drainage basins. Analyses of detrital zircons with U—Pb dating reveal a different signature for Ancestral Salt River Deposits (ASRD) as compared to the underlying basin fill. Trace element, $^{87}Sr/^{86}Sr$ ratios, and electron microprobe analyses of basalt fragments in the basal deposits of the ASRD in two different wells from Mesa, Arizona, show matches for outcrop sources near Bartlett Dam in the Verde drainage and near Stewart Mountain Dam in the Salt drainage. This indicates that the Salt and Verde rivers were transporting these basalts when the Salt River first flowed into the metropolitan Phoenix area. We employed tephrochronology to determine that the 3.3-Ma Nomlaki tuff accumulated in closed-basin playa deposits located near the present-day junction of the Salt and Verde rivers, providing a maximum-limiting age for the integration of both rivers. Because the age of mountains crossed by the Salt and Verde rivers pre-date <3.3 Ma by tens of millions of years, we rule out antecedence and superimposition as possible mechanisms to explain these transverse drainages. Multiple lines of evidence presented here are inconsistent with drainage piracy from headward erosion for both drainages: (i) headward erosion would have eroded analyzed basalt clasts from outcrop positions prior to drainage integration, and yet these clasts only occur in the lowest deposits of the ASRD; (ii) headward erosion would not be expected to create transverse streams in two distinct river drainages at the same time, and yet basalt clasts eroded from outcrops in the Salt and Verde rivers arrived together in the basal layer of the ASRD deposits, within the temporal resolution of 3 m sampling interval for well cuttings; (iii) headward erosion of the Verde River from the Nomlaki Tuff (providing maximum age of river integration at 3.3 Ma) to the breached Verde Formation-depositing lake at 2.5 Ma would require an extraordinarily fast rate of >12 cm/yr across multiple bedrock uplands; and (iv) Mescal Limestone clasts on the highest Salt River strath terrace cannot be explained by headward erosion. However, all analyzed evidence are consistent with the process of lake overflow. Based on our findings and the use of geomorphic criteria (Douglass et al., 2009), we conclude that lake overflow is the most likely cause of drainage integration of both the Salt River and the Verde River.

Contents

* Corresponding author.
E-mail addresses: ronald.dorn@asu.edu (R.I. Dorn), Axel.Wittmann@asu.edu (A. Wittmann), Matthjis.Vansoest@asu.edu (M. Van Soest).

https://doi.org/10.1016/j.geomorph.2020.107430
0169-555X/

1. Introduction

The Basin and Range province of western North America has long served as the type example of terrain formed by extensional deformation (Gilbert, 1928) with its core currently being the Great Basin defined by endorheic drainage. In the area now known as Arizona, through-flowing rivers originated in the Mogollon Highlands ca. 100 Ma and flowed south-to-north towards lowlands located at today's Colorado Plateau (Bilodeau, 1986). The onset of the San Andreas faulting changed plate tectonic dynamics from orogenic to collapsing crust in the Oligocene-Miocene in the Basin and Range of Arizona (Sonder and Jones, 1999). With this extension, closed-basins replaced the through-flowing drainages.

Well after the slowing and then cessation of Arizona extension about 16–9 Ma (Spencer and Reynolds, 1989; Fitzgerald et al., 1993), through-flowing drainages again developed across the region in the form of the Salt, Verde and Gila rivers (Melton, 1965). However, these new river systems now flow in the opposite direction towards the southwest, and they had to cross a series of closed depressions and bedrock highs.

In an analysis of alternative models of how rivers get across mountains and structural highs, Douglass et al. (2009) summarized geomorphic criteria used to discriminate between four alternative processes: antecedence; superimposition; drainage piracy; and lake overflow. Recent research in the Basin and Range Province of North America illustrates a renewed interest in the evolution of fluvial systems through the development of transverse drainages (Meek, 1989; Meek, 2004; Douglass et al., 2009; Larson et al., 2010; Roskowski et al., 2010; Spencer et al., 2013; Jungers and Heimsath, 2016; Meek, 2019). Prior research on the Rio Grande (Connell et al., 2005; Repasch et al., 2017) and lower Colorado (Pearthree and House, 2014; Howard et al., 2015) rivers emphasized the importance of lake overflow, whereas prior scholarship on Gila River drainages advocated piracy (Dickinson, 2015) and other processes (Jungers and Heimsath, 2016; Jungers and Heimsath, 2019). Besides research presented in this special issue, only two arguments have been made on how the Salt River integrated. Douglass et al. (2009) used geomorphic criteria to find that the Salt River originated by lake overflow across the Mazatzal Mountains near modern day Roosevelt Dam, and Dickinson (2015) included the Salt River as part of his model of Gila River prolongation by piracy via headward extension.

An important criteria used to adjudicate between competing hypotheses (Douglass et al., 2009) is the provenance of river sediments. Researchers use a wide variety of strategies for identifying the provenance of alluvium. Techniques employed include: dating of detrital zircons (Tripathy-Lang et al., 2013; Kimbrough et al., 2015; Repasch et al., 2017); tephrochronology (Dethier, 2001); dating of surficial volcanics such as basalts (Repasch et al., 2017); rare earth elements (Yang et al., 2006); isotopes of Pb (Zhang et al., 2014), Nd (Malusà et al., 2017), Sr (Talbot et al., 2000), or multiple isotopes (Roskowski et al., 2010; Vezzoli et al., 2010); trace elements (Collins et al., 1997; Malusà et al., 2017) measured by such techniques as inductively coupled plasma – atomic emission spectrometry (ICP-AES) (Mounteney et al., 2018); mineral assemblages in bulk samples (Vezzoli et al., 2016); and an understanding of unique rock types linked to geological mapping (Craddock et al., 2010).

An example of using multiple techniques to establish the provenance of river sediment comes from the only exoreic stream in the Basin and Range Province, outside of Arizona: the Rio Grande. The establishment an integrated Rio Grande river system is a story of progressive "top down" integration through a mixture of lake spillover events, building of volcanic fields, slowing rift extension and other processes. A key part of understanding the evolution of the Rio Grande involved a variety of methods including tephrochronology (Dethier, 2001), U—Pb detrital zircon chronology, and also understanding mapped geology sources (Repasch et al., 2017).

Laney and Hahn (1986) first mapped ancestral Salt River deposits (ASRD), using analyses from wells to identify a broad floodplain deposit in the eastern portion of metropolitan Phoenix, Arizona. Our research presents the first constraints on the provenance of this sediment. Like Repasch et al. (2017) we use the trace element composition of glass in tephra to obtain a maximum age on a key tephra unit, and we use U—Pb dating of detrital zircons to constrain the source regions of sediment. In addition, we collected basalt fragments from two wells drilled through the ASRD and into the basin fill beneath and use multiple strategies to try to correlate these fragments with potential source outcrops. We also used geologic mapping to source key gravel material found on the oldest strath terrace of the Salt River. The next section details the study area and sampling sites.

2. Study area and field collection strategy

Our study area is the region around the present-day junction of the Salt and Verde rivers, both immediately upstream and downstream (Fig. 1). Fig. 2 presents this area from two perspectives: an artistic, idealized interpretation of its late Pliocene appearance prior to drainage integration (Fig. 2A) and what the study area looks like today (Fig. 2B).

The modern-day junction of the Salt and Verde rivers (seen in Fig. 2B) occurs at the southern end of the lower Verde River valley. This once-closed depression was the site of playa accumulation (reddish silty-clay) called the Pemberton Ranch Formation (Skotnicki et al., 2003). Outcrops of this playa sediment are preserved at the surface protected by overlying alluvium, and one such exposure includes a welded tuff ("*Nomlaki" location identified in Fig. 2A in the

Fig. 1. The Salt and Verde rivers of central Arizona originate in the Mogollon Rim at the southern edge of the Colorado Plateau in Arizona. These two rivers, along with the Colorado and Rio Grande, form the only exoreic streams that cross the Basin and Range Province of western North America. This paper focuses on the area near the junction of these modern exoreic rivers. The framing of Figs. 2B and 7A are indicated as inset polygons.

Asher Hills at N 33.7284°, W 111.7190°), collected and analyzed for tephrochronology as a part of this research.

Prior to the arrival of the Salt and Verde rivers, the Phoenix metropolitan area hosted two major deep structural basins (Richard et al., 2007): the Luke Basin also called the West Salt River Basin and the Higley Basin also called the East Salt River Basin (Fig. 3) (Nations et al., 1982; Peirce, 1984; Spencer et al., 2001). These basins gradually filled up with sediment during the Pliocene, and it is likely that closed basins presented in Fig. 3 were in a state of "overfill" where sediment moved between basins via transport by ephemeral streams. However, no exotic or exoreic streams existed in the study area until the arrival of the Salt River gravels (Laney and Hahn, 1986).

The study area includes eastern metropolitan Phoenix, particularly the area of deposition of ancestral Salt River deposits (ASRD) that is identified in Fig. 2B. Skotnicki and DePonty (2020) present a compilation and analysis of well cuttings from Salt River Project drilling over the past several decades. Two of these wells and their cuttings are the focus of this research, located at the word "Wells" in Fig. 2B. Both wells are in Mesa, AZ, located near the intersection of Brown Road and Mesa Road (N 33.4371° W 111.8256°), and the other near the intersection of Lehi Road and Mesa Road (N 33.4583° W 111.8275°). Well cuttings were collected by drillers working with the second author. The second author hand-picked basalt clasts (Fig. 4) from different depths of these wells (samples collected every 10 ft or 3 m), and also collected bags of materials for the detrital zircon analyses.

We also carried out a field investigation collecting basalt samples from potential source outcrops of where the Verde River would have first traversed the bedrock high located around modern-day Bartlett Dam. These samples were collected from the area designated AB in Fig. 2A and B with specific locations noted in the results. Samples were also collected from where the Salt River would have first flowed in the area just below around modern-day Stewart Mountain Dam, designated as WH in Fig. 2A and B.

The search for possible outcrop sources of basalt was limited to the area downstream of the Stewart Mountain Dam (N 33.5514°, W 111.5480°) (Fig. 5) and downstream of Bartlett Dam (N 33.8178°, W 111.6359°) (Fig. 6). No matter whether the Salt and Verde rivers integrated by the process of lake overflow or piracy via headward extension, these locations would have been the first to experience fluvial erosion.

The area designated as "Wildhorse Gravels" in Fig. 5 is a deposit of gravels that includes at least three different types of basalt. These gravels rest on top of the north end of Péwé's (1978) Bush pediment and were identified as allochthonous gravels in Larson et al. (2010). The Wildhorse Gravels (abbreviated WH in figures and tables) originate from the Pass Mountain area to the east, but sources of two types of basalt in these gravels no longer exist. It is likely that the Wildhorse Gravels that remain today are remnants of a much thicker deposit. One of the WH basalts displays a texture of vesicles with abundant iddingsite, that when examined with a hand lens cannot be distinguished from gravels collected from the base of the ASRD (see WH in Fig. 4), and this sample was collected from N 33.5179°, W 111.6250°.

In the area designed as "A,B" in Fig. 6, we explored over 20 different potential basalt sources where the Verde River might have eroded basalt that was then transported to the two well sites. The Verde A and Verde B basalts come from the Needle Rock Formation (Skotnicki, 1996) that consists of subrounded basalt up to 0.8 m in diameter. We compared outcrop basalts to polished cross sections of basalt clasts hand-picked from the base of the ASRD. Only two outcrop locations were identified where basalts looked indistinguishable with a hand lens from the basal-ASRD gravels. These Verde A and Verde B boulders outcrop at N 33.7947°, W 111.6759° (Fig. 6). Some basalt clasts from the base of the ASRD and also the Verde A, B outcrop had notable textures discernable with a hand lens: small vesicles with plagioclase phenocrysts (labeled Verde A in Fig. 4); and large vesicles containing amygdales (labeled Verde B in Fig. 4).

The Lousley Hills (Fig. 6) contain Verde River alluvium with an abundance of basalt clasts. Gravels at the base of the Lousley Hills represent the oldest preserved sediment of the Verde River downstream of Bartlett Dam. Thus, it is possible that materials eroded from the Verde A-B site could have been deposited in these basal gravels. Therefore, basalt clasts were also collected at the base of the Lousley Hills at N 33.67797°, W 111.70856° that had textures similar to those extracted from the base of the ASRD (Verde A and Verde B in Fig. 4).

Basalt clasts were also collected from underneath the Gillespie shield volcano along the Gila River, west of metropolitan Phoenix. The Sentinel volcanic field was studied by Cave and Greeley (2004) and Cave (2015) for its age and relationship to the development of the lower Gila River. An $^{40}Ar/^{39}Ar$ age of 2.30 ± 0.35 Ma (Cave, 2015) for the Gillespie shield volcano at Cave's (2015) sample site S-06-180c provided an opportunity to evaluate basalt clasts in the alluvium underneath the dated basalt flow. Thus, basalt alluvium was examined in the field at this site the same way as the other field sites, and three clasts that had a hand lens texture indistinguishable from Verde B (see Fig. 4) were collected for trace element and strontium isotope measurements.

A different provenance field investigation focused on where the Salt River passes through the Mazatzal Mountains after leaving the Tonto Basin (Fig. 7). The region around modern-day Roosevelt Dam contains abundant outcrops of the Mescal Limestone (Spencer and Richard, 1999), but this limestone does not appear anywhere downstream of the Roosevelt Dam area. Regardless of whether the Salt River integrated across the Mazatzal Mountains via headward extension (Dickinson, 2015) or lake overflow (Douglass et al., 2009), it would have eroded the Mescal Limestone. A headward eroding Salt River would have reached this area only just prior to breaching into the Tonto Basin (see Fig. 7). An overflowing Salt River. however, would have eroded this area first and the material would have

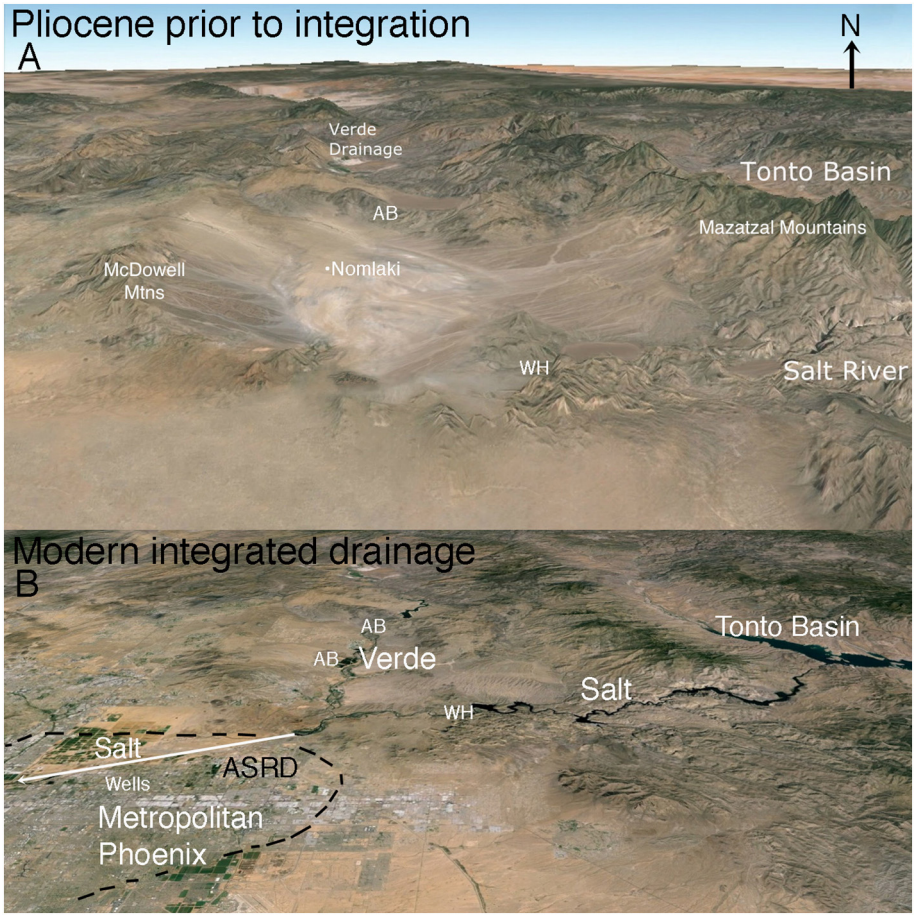

Fig. 2. Geomorphic context of the sampling sites located in the northeastern portion of the present-day Phoenix metropolitan region. Image A is an artistic reconstruction of what the study area could have looked like some 4 Ma prior to drainage integration. Image A is centered on the lower Verde River valley that was bounded by the McDowell Mountains on the west, the Mazatzal Mountains on the east, and the Usery Mountains on the south. Nomlaki identifies the location of the tephra sample from playa deposits that occupied the lower Verde basin. A,B identify the outcrop location of Verde River basalt samples A and B. WH identifies the outcrop location of the Wildhorse basalt sample. Image B is a modern Google Earth image that also identifies the position of the modern-day Verde and Salt rivers, as well where the Salt River flows dry through Metropolitan Phoenix. The dashed black lines indicate the extent of the Ancestral Salt River Deposits (ASRD), and "Wells" indicates the position of the two wells where drill cutting were analyzed. In these oblique images, the lower boundaries are ~40 km and ~ 60 km across.

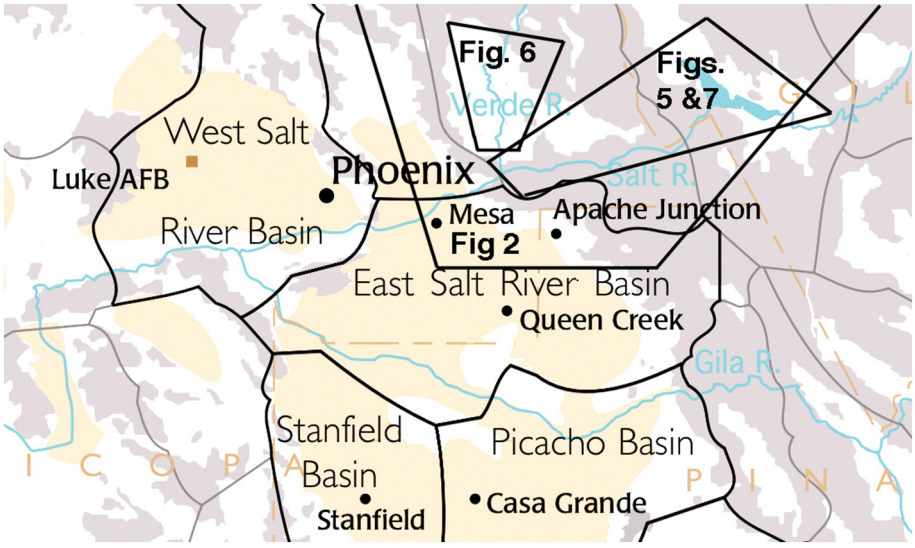

Fig. 3. Groundwater basins in the study area that reflect deep structural basins. The Gila, Salt, and Verde rivers traverse the Picacho, East Salt River, and West Salt River groundwater basins. We also consider the West Salt River Basin synonymous with the Luke structural basin and the East Salt River Basin synonymous with the Higley structural basin. Other polygons indicate the approximate framings of Figs. 2, 5 and 7. The figure is modified from the U.S. Geological Survey.

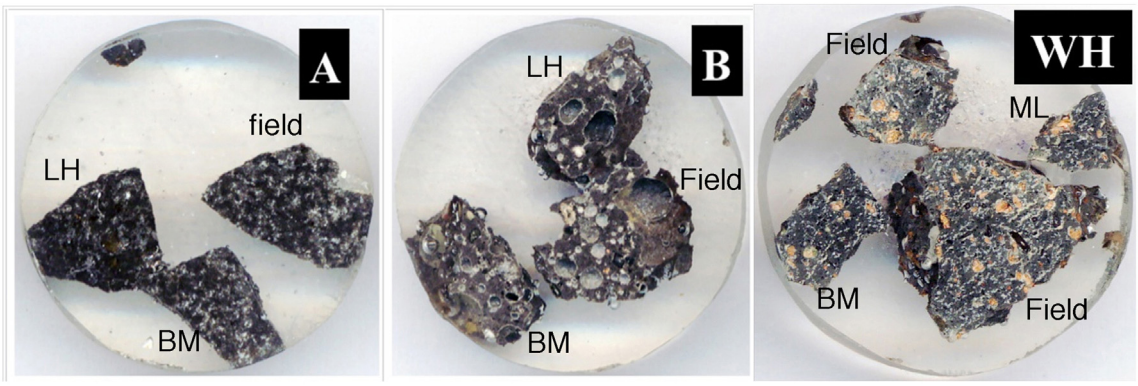

Fig. 4. Optical image of the Verde River and Salt River basalts that have a similar appearance to basalt fragments collected from Salt River Project (SRP) well deposits. A and B refer to Verde River field outcrops A and B. Wildhorse refers to the Wildhorse gravel field area next to the Salt River. Note the particularly large vesicles in Verde B samples, the iddingsite replacing olivine in WH samples, and the smaller vesicles in Verde A samples. BM refers to samples picked out from the base of ancestral Salt River gravels in the Brown and Mesa well; ML refers to samples picked out from the base of ancestral Salt River gravels in the Mesa and Lehi well; field refers to outcrop samples; and LH refers to samples collected from the base of the Lousley Hills gravel deposits.

been among the first to be transported downstream. Thus, we carried out extensive fieldwork to look for evidence of Mescal Limestone deposits on the oldest possible terrace of the Salt River: the hypothesized Stewart Mountain Terrace (Larson et al., 2010), even though no Mescal limestone occurs in any of the lower Salt River terraces (Kokalis, 1971; Péwé, 1978).

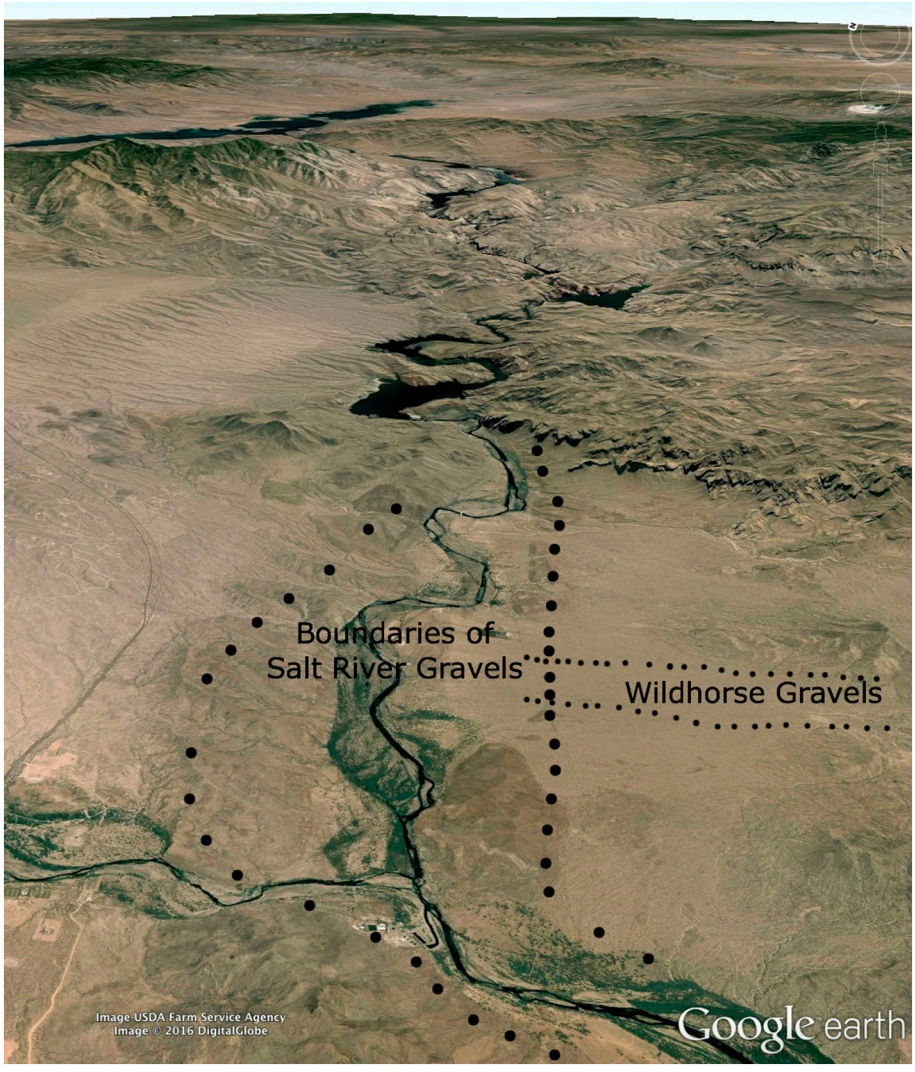

Fig. 5. In this northeast-looking Google Earth view with a framing indicated on Fig. 3, black dots identify the extent of Salt River gravels. While the location of the Salt River has changed over time, the Wildhorse (WH) gravels would have occupied the low spot in the landscape and would have eroded when the Salt River first started flowing through the area.

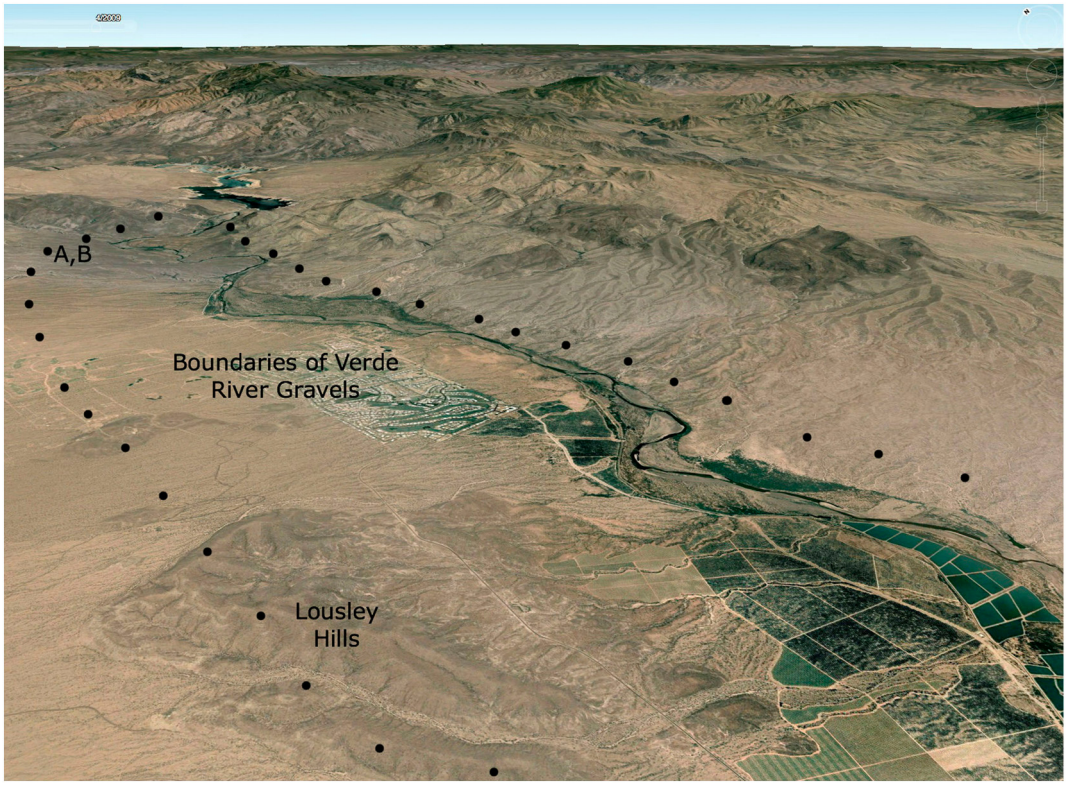

Fig. 6. In this north-looking Google Earth view, with a framing indicated on Fig. 3, the black dots indicate the extend of the Verde River gravels. When the Verde River first flowed across the position now occupied by Bartlett Dam and started depositing the Lousley Hills gravels, the physical extent of these gravels was likely much greater and could have constituted an elongated alluvial fan. A possible original path of the Verde River was likely west of its present-day position. Then, over time, the Verde shifted to the east. The samples analyzed as potential source basalts were collected at the A,B location beneath the Bartlett Dam site.

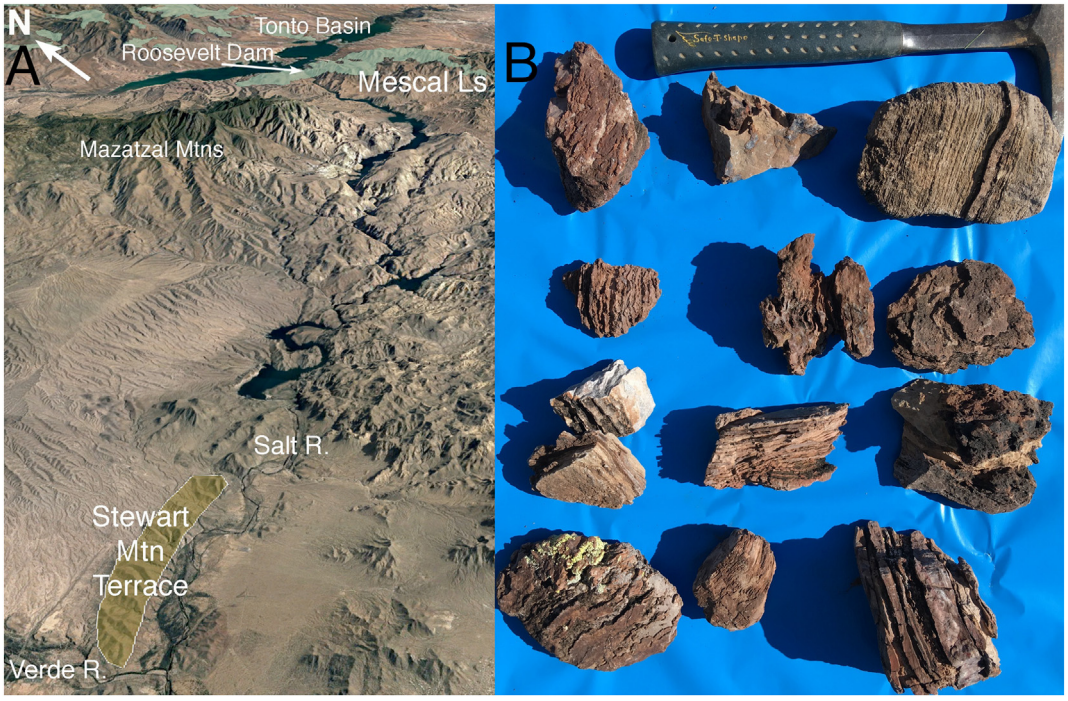

Fig. 7. Image A shows a northeast-looking view via Google Earth, with a framing shown in Fig. 3, the Salt River starts its journey through the fault block of the Mazatzal Mountains at the present-day location of Roosevelt Dam. There, the Salt River encounters a large outcrop of Mescal Limestone (identified in shading around Roosevelt Dam). Although the Mescal Limestone outcrops elsewhere above Roosevelt Dam, it does not occur between this location and the Stewart Mountain Terrace. Thus, the only known source of the displayed clasts of Mescal Limestone, collected from the surface of the Stewart Mountain Terrace, is the Roosevelt Dam area. Image B shows the distinctive appearance of Mescal Limestone clasts after the carbonate has dissolved and the silicified components stand out. These samples were collected from the surface of the Stewart Mountain Terrace (Larson et al., 2010) whose position is indicated in Image A. The clasts are best explained by the presence of the Salt River at this location soon after the overflow event.

3. Methods

3.1. Tephrochronology

Playa deposits in the lower Verde River valley (the Pemberton Ranch Formation, Skotnicki et al., 2003) contain a ~30-cm-thick tephra deposit (N 33.7279°, W 111.7007°). Its deposition must pre-date integration of the Verde and Salt rivers, because the tephra was deposited on and buried by closed-basin playa deposits. This playa occupied a deep bedrock basin now found just north of the confluence of the Salt and Verde rivers. A careful examination of 10 polished tephra samples with back-scattered electron microscopy revealed that most of the glass has thoroughly altered. However, a small percentage of intact glass shards were found and 30 were analyzed by the JEOL JXA-8530F electron microprobe using a 5 μm beam diameter, 5 nA, and 15 kv. The microprobe measurements were then compared with known tuff deposits in the Basin and Range Province of Arizona, such as Lava Creek B ash at 0.62 Ma (Izett and Wilcox, 1982), Bishop Creek ash at 0.74 Ma (Sarna-Wojcicki et al., 2005), Nomlaki tuff at 3.3 Ma (Poletski, 2010), the Lawlor Tuff at 4.8 ma (Sarna-Wojcicki et al., 2011), and the Connant Creek ash at ca. 5.5 Ma (Morgan and McIntosh, 2005).

3.2. Collection of samples from wells

The detrital zircon (DZ) and the basalt provenance research started with subsurface Salt River Project (SRP) well cuttings. The DZ samples came from the Brown and Mesa well (Fig. 8), whereas the picked out individual basalt clasts came from both the Brown and Mesa and Mesa and Lehi wells (Fig. 8). For the basalt provenance research, although typically comprising less than a few percent of the clasts within an interval of cuttings, basalt clasts were collected from well cuttings by hand from a variety of different depth intervals (Fig. 8) for subsequent laboratory analyses.

3.3. Detrital zircon analyses

Zircons are small accessory minerals that crystallize in igneous rocks and are reliable geochronometers because they include traces of uranium. Upon erosion of these rocks, mineral grains lack a distinct cleavage and hence are robust. They are also resistant to the most common chemical weathering agents and therefore are preserved long after most other mineral grains. Their presence and age profile in sediment can provide a very useful 'fingerprint' of the source area (s) for the sediment (Tripathy-Lang et al., 2013; Kimbrough et al., 2015; Repasch et al., 2017). For our study, the two samples analyzed for detrital zircons (DZ) came from the Brown and Mesa well (Fig. 8) from depths below the surface: 170 ft (52 m) ASRD gravels; and 310 ft (95 m) in 'basin-fill' deposits below the ASRD.

Detrital zircons were separated from the well cuttings using standard methods (Tripathy-Lang et al., 2013). U—Pb analyses of 150 individual zircons in each sample were prepared and analyzed at the Noble Gas Geochronology and Geochemistry Laboratory (KVH Group) at Arizona State University. Backscattered electron images for mounted and polished crystals helped identify appropriate locations for targeting the center of an ablation pit. They were then analyzed by methods detailed in Tripathy-Lang et al. (2013).

3.4. Basalt Provenance analyses

Volcanologists (Óladóttir et al., 2011) and archaeologists examining basalt tools (Gluhak and Rosenberg, 2018) use major, minor, and trace element geochemistry to determine potential sources, including from north-central Arizona quarries (Linthout, 2015; Rosenberg et al., 2015; McAlister and Allen, 2017), where Ti, Fe, Rb, Sr, Y, Zr and Nb were particularly effective in differentiating different potential quarry areas (Fertelmes and Glascock, 2018). Small-scale basaltic systems like those in the study area with small volumes of magma can experience different and complex processes that are not seen in larger volume systems. This can lead to significant compositional variety that reflects melting processes at different depths, a range of melting proportions, heterogeneous sources, and mixing in a small plumbing system (McGee and Smith, 2016).

Given this success in establishing provenance for basalt tools, we sequenced different strategies to assess potential linkages between basalt clasts removed from well cores to potential field outcrops. (i) Clasts from the base of the ASRD in the two wells were taken into the field to visually compare them (using a hand lens) with different basalt outcrops in the Salt and Verde drainages. If an outcrop sample had a hand lens texture indistinguishable from a well sample (e.g., vesicles with abundant iddingsite seen in WH and other textures in Verde A,B in Fig. 4), then, (ii) inductively coupled plasma atomic emission spectrometry (ICP-AES) analyses were completed by ALS Minerals, after pulverizing portions of individual basalt clasts to <75 μm and four acid treatment Code ME-ICP61 that analyzes 33 elements. These analyses were completed on all 69 basalt clasts collected from well õ-cuttings, 14 basalt clasts from the Verde A-B outcrop, seven basalt clasts from Wildhorse gravels, and eight basalt clasts from the base of the Lousley Hills Verde River terrace. We also analyzed the trace element suite of three basalt clasts from underneath the Gillespie shield volcano with an $^{40}Ar/^{39}Ar$ age of 2.30 Ma ± 0.35 (Cave, 2015). Geographic coordinates of all locations are presented in results.

For those samples with similar suites of trace elements, we then (iii) used electron wavelength dispersive electron microprobe analysis (EMPA) to compare the compositions of plagioclase and pyroxenes from the different samples. Also for samples with similar suites of trace elements, (iv) we qualitatively examined back-scattered electron microscopy (BSE) and cathodoluminescence (CL) textures (Krinsley et al., 2005; Scholonek and Augustsson, 2016). For the trace element and textural assessments, we used electron microprobe analysis with the JEOL JXA-8530F at Arizona State University. Also for samples with similar suites of trace elements, we used (v) $^{87}Sr/^{86}Sr$ ratios that can differ among basalts, including those in central Arizona (Leeman, 1970; Leeman, 1982; Wittke et al., 1989). Thus, split samples from outcrop positions analyzed for trace elements were analyzed for $^{87}Sr/^{86}Sr$ ratios. Similarly, split samples from basalt clasts sampled from the two wells were analyzed for $^{87}Sr/^{86}Sr$ ratios.

3.5. Mescal Limestone Provenance

Field reconnaissance of the Stewart Mountain Terrace of the Salt River (Larson et al., 2010) assessed the presence and abundance of Mescal Limestone clasts at the terrace surface. The Mescal Limestone is part of the Middle Proterzoic Apache Group. The only known bedrock location of the Mescal Limestone west of the Tonto Basin is right around the area of the present day location of Roosevelt Dam (Spencer and Richard, 1999). The outcrop is quite extensive and the mapping unit is overlain on a Google Earth frame in Fig. 7.

If the Salt River had integrated across the Mazatzal Mountains fault block through lake overflow at the present-day area of Roosevelt Dam, it would have first eroded the Mescal Limestone from this area. In contrast, if the Salt River integrated across the Mazatzal Mountains via headward extension, the last clasts to have eroded would have been the Mescal Limestone. A river extending headward from the location of this terrace up into the Mazatzal Mountains (Fig. 7) would have incised into the terrace because of the evolution of its longitudinal profile (Larson et al., 2010) and hence Mescal Limestone should occur in lower Salt River terraces, if at all. Thus, we undertook a more extensive survey of the surface of the Stewart Mountain Terrace to look for Mescal Limestone clasts, because the Stewart Mountain Terrace is hypothesized to be where the Salt River flowed through the study area after its initial integration (Larson et al., 2010).

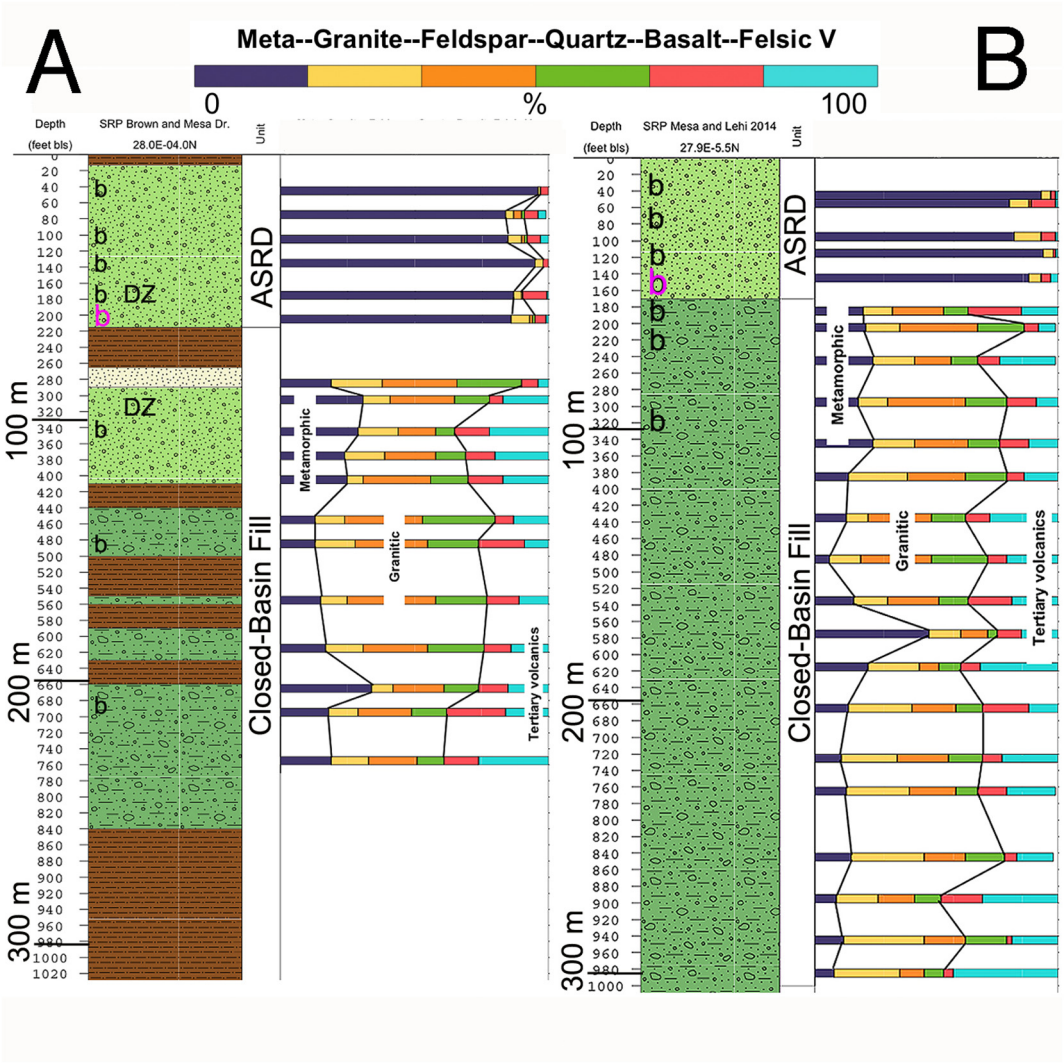

Fig. 8. Mineralogic logs of cuttings from wells where samples were analyzed for basalt provenance (identified by letter "b") and detrital zircons (identified by "DZ"). A is the log from a Salt River Project well near the intersection of Brown Drive and Mesa Drive in Mesa, Arizona. B is the log from a Salt River Project well near the intersection of Mesa Drive and Lehi Drive in Mesa, Arizona. ASRD indicates the ancestral Salt River deposits. Depths are both meters and also feet below the surface; feet is used in well drilling operations. The purple-shaded "b" indicates the only depth where the ICP trace elements and electron microprobe data are consistent with possible source outcrops in the Verde and Salt river drainages. The colour-coded lithologic key emphasizes that the ASRD deposits are dominated by metamorphic clasts, especially quartzite. Light green shading indicates a coarse composition interpreted as being the ASRD. Darker green shading indicates other sandy and gravel-containing sediment. Brown shading indicates fine sediment dominated by clay and silt with some sand. Red shading indicates playa deposits of clay and silt. White with fine stipples indicates sand that is perhaps aeolian.

4. Results

4.1. Tephrochronology analyses

Table 1 presents analyses of 30 separate glass shards in the Asher Hills tuff (see •Nomlaki in Fig. 2A for context). After comparison with known tuff deposits in the Basin and Range Province of Arizona, namely the Lava Creek B ash at 0.62 Ma (Izett and Wilcox, 1982), Bishop Creek ash at 0.74 Ma (Sarna-Wojcicki et al., 2005), the Lawlor Tuff at 4.8 Ma (Sarna-Wojcicki et al., 2011), and the Connant Creek ash at ca. 5.5 Ma (Morgan and McIntosh, 2005), data in Table 1 matched microprobe analyses of glass shards of the Nomlaki Tuff eruption approximately 3.3 Ma (Poletski, 2010). We have not found any other deposits of the Nomlaki Tuff in the study area.

The existence of any Verde River at 3.3 Ma would have meant that the playa no longer existed and the tuff could not occur interbedded with playa deposits. Thus, the Verde River must have integrated after 3.3 Ma. These findings also reveal that the Lousley Hills gravel deposits (Fig. 6) that rest on top of the playa sediments and ash are younger than 3.3 Ma.

4.2. Detrital zircon analyses

Samples were analyzed from the Brown and Mesa Well (Fig. 8) that contains two distinct gravel types: (1) ASRD above 215 ft (66 m), and (2) basin-fill deposits below 215 ft (66 m). For both samples, Fig. 9 shows the probability density plot showing the age distribution of detrital zircon ages >400 Ma, and Fig. 10 shows the probability density plot showing the distribution of detrital zircon ages between 0 and 80 Ma. We found no ages between 80 and 400 Ma. All 150 U-Pb zircon ages are plotted in Figs. 9 and 10. The more ages that fall within a particular narrow age range, the taller the peak on the graph. Therefore, the taller peaks indicate that more zircons exist in the cuttings of that age range. Both figures show the relative probability of the ages, and not the absolute number.

The 8 Ma peak in the ASRD deposits (Fig. 10) could potentially derive from extensive basalts in the present-day Verde drainage basin, but we are not aware of literature containing precise dating of volcanics with ages in the 9–11 Ma range found in the basin fill. However, ongoing research into the Tertiary volcanic history of

Table 1
Electron microprobe analyses of individual glass shards in the Asher Hills ash site compared to the Nomlaki tuff (Poletski, 2010). The values are weight percent, and standard deviation is reported as 1 sigma.

Shard	Na_2O	MgO	Al_2O_3	SiO_2	K_2O	CaO	TiO_2	MnO	FeO	BaO	Total
1	3.59	0.26	12.90	72.7	3.53	1.11	0.24	0.06	1.08	0.05	95.54
2	3.67	0.10	13.31	74.0	3.54	0.93	0.19	0.02	0.53	0.11	96.41
3	3.64	0.17	13.01	74.5	3.53	1.05	0.29	0.05	0.84	0.15	97.21
4	3.70	0.17	12.74	74.5	3.44	1.06	0.30	0.04	1.09	0.09	97.12
5	3.62	0.24	12.86	74.5	3.27	1.14	0.24	0.05	1.05	0.16	97.15
6	3.69	0.21	13.11	74.0	3.28	1.01	0.22	0.05	0.97	0.18	96.75
7	3.57	0.24	13.03	73.4	3.07	1.24	0.26	0.03	1.06	0.11	96.00
8	3.62	0.09	13.04	73.9	3.55	0.98	0.29	0.02	0.83	0.13	96.44
9	3.54	0.06	12.92	73.3	3.38	1.07	0.27	0.06	0.96	0.19	95.79
10	3.64	0.12	13.12	73.1	3.29	1.20	0.25	0.05	0.86	0.08	95.68
11	3.43	0.17	13.27	73.2	3.62	0.97	0.29	0.04	0.82	0.12	95.94
12	3.52	0.21	12.52	73.8	3.51	1.00	0.21	0.05	0.90	0.12	95.84
13	3.61	0.27	12.94	73.6	3.34	1.27	0.27	0.04	1.13	0.11	96.59
14	3.70	0.17	12.98	73.1	3.71	1.33	0.29	0.03	0.87	0.05	96.27
15	3.83	0.27	13.31	73.0	3.03	1.26	0.31	0.02	1.33	0.26	96.63
16	3.85	0.23	13.08	73.6	3.08	1.02	0.23	0.05	1.07	0.02	96.22
17	3.65	0.23	12.99	73.3	3.28	1.06	0.24	0.10	1.06	0.22	96.09
18	3.69	0.26	13.16	73.8	3.20	1.13	0.25	0.08	1.01	0.24	96.82
19	3.92	0.23	12.83	74.0	3.24	1.10	0.25	0.05	1.01	0.04	96.69
20	3.78	0.14	12.55	74.00	3.29	1.08	0.27	0.02	1.25	0.06	96.43
21	3.72	0.20	13.13	73.5	3.33	1.21	0.26	0.11	1.30	0.03	96.79
22	3.84	0.25	13.38	74.5	2.90	1.11	0.24	0.04	1.12	0.29	97.63
23	3.83	0.17	12.92	73.6	3.28	1.40	0.17	0.02	1.07	0.05	96.48
24	3.76	0.34	13.24	73.2	3.38	1.36	0.24	0.02	1.35	0.11	96.95
25	3.84	0.09	13.17	73.5	3.82	1.19	0.21	0.05	1.05	0.12	97.00
26	3.91	0.17	13.12	73.1	3.69	1.33	0.19	0.00	1.37	0.02	96.88
27	3.92	0.30	13.09	73.8	3.19	1.32	0.24	0.03	1.17	0.13	97.14
28	3.95	0.29	13.05	74.0	3.16	1.26	0.29	0.03	1.28	0.17	97.44
29	3.76	0.18	12.75	73.2	3.50	1.29	0.16	0.04	1.00	0.00	95.88
30	3.63	0.25	12.71	73.2	3.20	1.13	0.25	0.06	1.15	0.21	95.77
Mean	3.71	0.20	13.01	73.6	3.35	1.15	0.25	0.04	1.05	0.12	96.5
Standard Deviation	0.13	0.07	0.21	0.49	0.21	0.13	0.04	0.02	0.19	0.08	0.56
					Poletski, 2010						
Mean	3.76	0.21	13.17	73.4	3.31	1.22	0.26	0.05	1.07		96.43
Standard Deviation	0.26	0.05	0.19	0.62	0.22	0.05	0.03	0.03	0.12		0.59

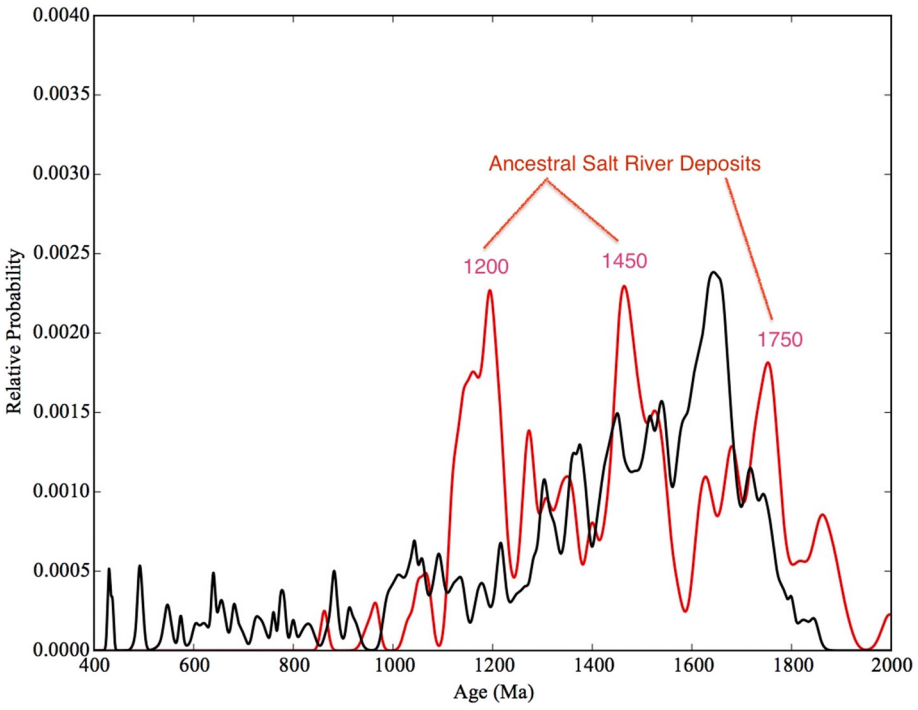

Fig. 9. Probability Density Plot showing the age distribution of detrital zircon for ASRD (in red) and the underlying basin-fill deposits (in black) for the time period from 400 to 2000 million years; 150 samples were analyzed for both materials.

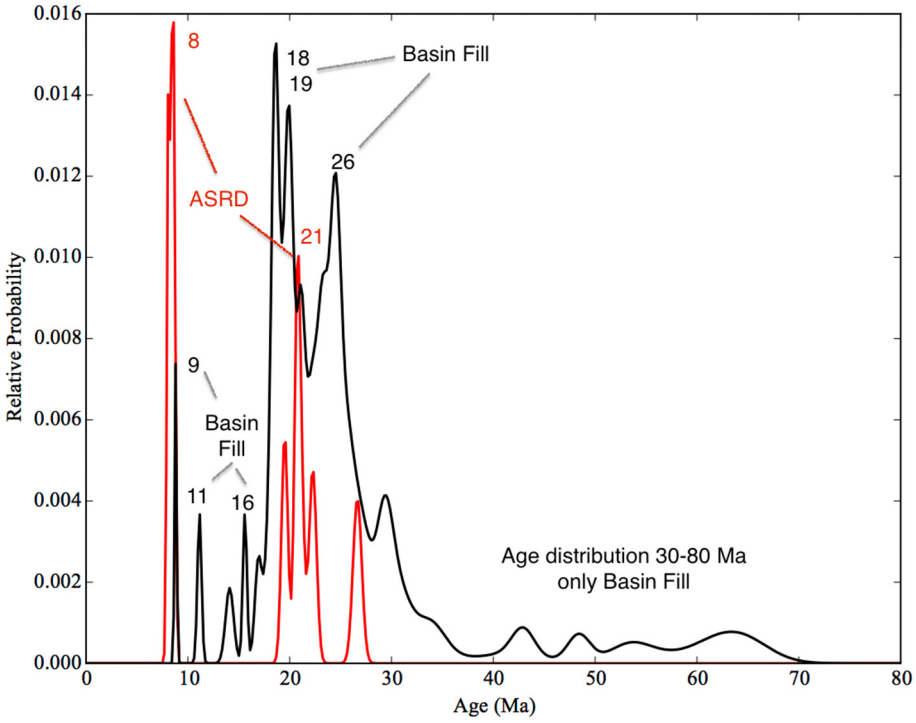

Fig. 10. Probability Density Plot showing the age distribution of detrital zircon ages 0–80 Ma for ASRD (in red) and the underlying basin-fill deposits (in black); 150 samples were analyzed for both materials.

central Arizona will allow a refined interpretation of these relatively recent zircon ages. The 16 Ma peak in the basin fill could derive from basalts and andesites of this age (Shafiqullah et al., 1980) found in the East Salt River (Higley) Basin (Fig. 3).

The basin-fill deposits contain a large peak centered between 18 and 19 Ma. This is the age of most of the magmatism in the Superstition/Superior volcanic field (Skotnicki and Ferguson, 1996; McIntosh and Ferguson, 1998). In contrast, the ASRD contain a smaller peak centered near 21 million years that could be associated with late Superstition eruptions (Shafiqullah et al., 1980)

The basin-fill deposits contain zircons between 30 and about 850 Ma, but the ASRD do not. This age range represents the early Tertiary, Mesozoic, Paleozoic, and the Neoproterozoic. Arizona contains abundant sedimentary rocks from these time periods, but very few igneous rocks from these time periods. However, zircons with these ages are widespread within Late Cretaceous sedimentary rocks and could represent grains that were recycled from igneous activity farther west and north (Leier and Gehrels, 2011). Therefore, the basin-fill deposits probably contain material that has been recycled from older Mesozoic and Paleozoic rocks but the analyzed ASRD sediments do not.

ASRD deposits show a large peak near 1200 Ma. This corresponds well to published detrital zircon ages (Stewart et al., 2001) from the Dripping Spring Quartzite and from the Troy Quartzite, both of which have widespread outcrops in the Salt River watershed. Although the basin-fill deposits have this pronounced peak, some of the material could have derived some of the Salt River watershed.

Peaks near 1450 Ma for the ASRD and basin fill are probably derived from widespread granites of this age that occur both locally around the closed basin and much farther away, east of the Mazatzal Mountains. Both deposits show a peak near 1650 Ma, though the peak for the ASRD is much smaller. Granites of this age are exposed around the closed basin and as far east as Four Peaks (Skotnicki, 2000), but only one granite of this age is known farther east near Young, Arizona (Labrenz and Karlstrom, 1991).

4.3. Basalt provenance analyses

4.3.1. Overview of basalt analyses

The basic finding presented in this section is that trace element, $^{87}Sr/^{86}Sr$ ratios and petrologic measurements are consistent with the hypothesis that basalt fragments from the Salt and Verde watersheds arrived at the same time in the basal deposits of the ASRD in two different wells (see Fig. 8).

To increase confidence in this finding, provenance tests need to be run on the dozens of basalt sources upstream of the overflow locations at Bartlett Dam on the Verde and Stewart Mountain Dam on the Salt drainages. However, the magnitude of that effort is beyond the scope of this research project.

4.3.2. ICP-AES trace element analyses

Fig. 11 presents scattergraphs of different geochemical relationships of all of the basalt analyses that are representative of the full geochemical data set of ICP-AES analyses (Supplemental File 1). Fig. 11 illustrates the typical clustering and also spread among the analyses. The Wildhorse (WH) gravel match between source and ASRD is the clearest match making it likely that the WH gravel is the source of the basalt clasts found in the base of the ASRD deposits. The Verde B gravel shows the second clearest match between potential outcrop source and basalt clasts in the deepest depths of the ASRD deposit. The Verde A grave shows the third clearest match between outcrop and well drillings.

We extracted 13 basalt clasts from the Brown and Mesa well at depths ranging from 50 to 180 ft (15–55 m) above the base of the ASRD and 13 basalt clasts from the Mesa and Lehi well at depths ranging from 50 to 150 ft (15–46 m) (identified by black 'b' in Fig. 8) that have a trace element composition that matches the analyzed outcrops. In addition, no geochemical matches to outcrop samples occurred in the 12 basalt clasts from the basin fill beneath the ASRD in the Brown and Mesa well and 10 basalt clasts from the basin fill beneath the ASRD in the Mesa and Lehi well.

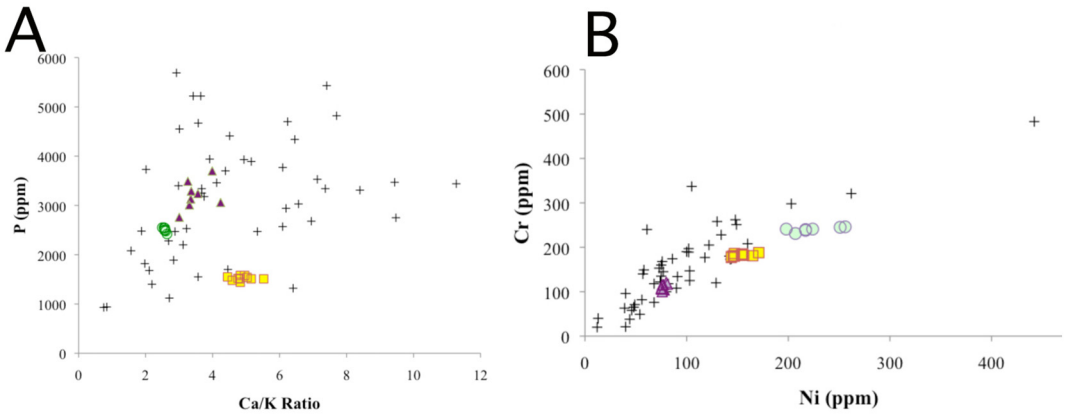

Fig. 11. ICP analyses of every basalt fragment analyzed ($n = 98$). The circles are the Wildhorse gravels from outcrop and base of the ASRD. The triangle and squares are Verde A and B basalts from the outcrop, respectively, Lousley Hills and base of the ASRD. The + symbols are all of the basalt samples that do not show geochemical similarities. Additional geochemical analyses are available in Supplemental File 1.

The only geochemical matches between outcrop and well cuttings existed in the base of the ancestral Salt River gravels at 200–210 ft (61–64 m) in the Brown and Mesa Well and 180–190 ft (55–58 m) in the Mesa and Lehi well. Only 11 of the 23 basalt clasts from these depths matched outcrop basalt geochemistry, while 12 basalt clasts from these depths did not have a geochemical match. The drill cuttings are extracted at 10 ft (3 m) intervals, and it is not possible to distinguish whether the WH (Salt River) or Verde A,B (Verde River)-sourced basalts were older.

The two other field sites with river gravels that were sampled also showed a geochemical match to Verde outcrop samples. As noted earlier, Verde A samples are notable for their small vesicles with plagioclase phenocrysts (labeled Verde A in Fig. 4); and Verde B samples are characterized by large vesicles containing amygdales (labeled Verde B in Fig. 4). Of the eight basalt clasts removed from the contact of the Verde River gravels and the underlying Pemberton Ranch playa deposits that appeared to have hand lens textures similar to Verde A and Verde B, two had geochemical matches to Verde B and two matched Verde A outcrop samples. (Supplemental File 1). The three basalt clasts with large vesicles containing amygdales sampled from underneath the Gillespie volcano basalt have a geochemical match with the Verde B outcrop, Verde B cobbles in the two wells, and Verde B cobbles from the base of the Lousley Hills (Supplemental File 1).

4.3.3. $^{87}Sr/^{86}Sr$ ratios

Table 2 presents $^{87}Sr/^{86}Sr$ ratios for basalts from source outcrops, well samples, and river gravel deposits at the base of the Lousley Hills and underneath the Gillespie volcano. $^{87}Sr/^{86}Sr$ ratios for basalts from Needle Rock Formation (Skotnicki, 1996), including the Verde A and Verde B basalts identified by trace elements, have ratios in the low 0.706 range. This is true for the Wildhorse gravel, but the other sampled basalt gravels at the Wildhorse location (Fig. 3) have ratios in the mid 0.705 range. The basalt clasts from underneath the 2.30 ± 0.35 Ma Gillespie shield volcano adjacent to the Gila River had virtually identical $^{87}Sr/^{86}Sr$ ratios ranging from 0.70622–0.70627 (Table 2).

In contrast, $^{87}Sr/^{86}Sr$ ratios for basalt clasts removed from the wells show a substantial range. Those basalt clasts above the base of the ASRD have lower ratios centered around 0.704. In contrast, basalt clasts in the basin fill below the ASRD center around ratios that are the lowest ~0.703. The results presented in Table 2 are important only from the perspective that they do not contradict the hypothesis that clasts from the Verde and Salt drainages arrived at the same depth in two wells.

4.3.4. Electron microprobe analyses

Electron microprobe analyses were conducted on all of the samples seen in Fig. 4. We focused on characterizing the major and minor element composition of pyroxene and plagioclase phenocrysts. High precision and accuracy wavelength dispersive electron microprobe analyses of pyroxene and plagioclase minerals of the Verde A, Verde B, and Wildhorse materials show clustering that is consistent with the trace element finding reported in Section 4.3.2 and the strontium isotope results in Section 4.3.3 (Figs. 12 and 13). The number of pyroxenes analyzed in each sample (source, terrace deposit, ASRD deposit), however, could be increased further for statistical testing. At this point these microprobe tests do not conflict with the notion that the Salt and Verde rivers arrived at the same time.

Cathodoluminescence (CL) and back-scattered electron (BSE) images were used to examine the textures of basalt clasts. CL is induced by the excitation of electrons in a non-metallic sample from the valence band to the conduction band caused by the incidence of electrons. Once these electrons return to their original state, the surplus energy can be dissipated as photons in the visible wavelength range, causing luminescence. Crystal-structure defects or trace elements are the main causes for cathodoluminesence, which can be useful in concert with BSE images to characterize petrographic characteristics and even provenance (Brokus et al., 2015; Scholonek and Augustsson, 2016). Fig. 14 presents a summary of the Cl and BSE properties of selected basalt clasts – with the same finding: basalts in the basal layers of the ASRD have their source at outcrops in the Salt and Verde watershed, with the implication that the Salt and Verde rivers arrived at the same time.

4.3.5. Summary of basalt testing

Although none of the results provide unequivocal evidence of a penecontemporaneous arrival of the Salt and Verde rivers, the findings presented in this section do point to outcrop sources for basalts found in the base of the ASRD that derive from both the Salt and the Verde watersheds. We also think it possible that the Verde A,B geochemical and strontium-isotope matches between bedrock outcrops gravels at the base of the Lousley Hills indicate a source-deposit connection, just as the Verde B geochemical and strontium match basalt gravels underneath the Gillespie basalt flow.

We do not view the results as conclusive, but rather that trace element, strontium isotope, and petrologic data are consistent with the penecontemporaneous integration of the Salt and Verde rivers. The biggest challenge to future research in this direction is that the number and variety of basalts in central Arizona are widespread, and the scope of falsifying these other basalts as sources is well beyond the scope of this research project.

4.4. Mescal limestone provenance

A survey of the surface of the Stewart Mountain Terrace (see Fig. 7) revealed the presence of scattered clasts of Mescal Limestone. The

Table 2
$^{7Sr}/^{86}Sr$ ratios for basalts from outcrop locations and also from basalt clasts from well cuttings at different depths in the Brown and Mesa and Mesa and Lehi wells (sampling depths shown in Fig. 8). Bold indicates Verde A, Verde B, and Wildhorse (WH) samples from outcrop positions and those with similar trace element suites found in the base of the ASRD. "No outcrop match" means that the basalt clast did not have a trace element signature that was a match between outcrop and well cutting materials. By convention, uncertainties are not reported for single isotope measurements.

Basalt field outcrop	Location	Trace element outcrop match	$^{87}Sr/^{86}Sr$
Verde R. below Bartlett Dam	N33.7947° W111.6759°	No outcrop match	0.70607
Verde R. below Bartlett Dam	N33.7947° W111.6759°	No outcrop match	0.70632
Verde R. below Bartlett Dam	N33.7947° W111.6759°	No outcrop match	0.70556
Verde R. below Bartlett Dam	N33.7947° W111.6759°	No outcrop match	0.70601
Verde R. below Bartlett Dam	N33.7947° W111.6759°	No outcrop match	0.70628
Verde R. below Bartlett Dam	N33.7947° W111.6759°	No outcrop match	0.70566
Verde R. below Bartlett Dam	N33.7947° W111.6759°	Verde A	0.70597
Verde R. below Bartlett Dam	N33.7947° W111.6759°	Verde A	0.70641
Verde R. below Bartlett Dam	N33.7947° W111.6759°	Verde B	0.70623
Verde R. below Bartlett Dam	N33.7947° W111.6759°	Verde B	0.70621
Salt R. Wildhorse Gravels	N33.7947° W111.6759°	WH	0.70613
Salt R. Wildhorse Gravels	N33.7947° W111.6759°	WH	0.70625
Salt R. Wildhorse Gravels	N33.7947° W111.6759°	No outcrop match	0.70554
Salt R. Wildhorse Gravels	N33.7947° W111.6759°	No outcrop match	0.70523
Salt R. Wildhorse Gravels	N33.7947° W111.6759°	No outcrop match	0.70574
Salt R. Wildhorse Gravels	N33.7947° W111.6759°	No outcrop match	0.70543
Cave (2015) S—06180C site	N33.0043° W113.1736	Verde B	0.70622
Cave (2015) S—06180C site	N33.0043° W113.1736	Verde B	0.70627
Cave (2015) S—06180C site	N33.0043° W113.1736	Verde B	0.70625
Salt river well	**Depth in well**	**Trace element signature**	**$^{87}Sr/^{86}Sr$**
Brown&Mesa	40–50	No outcrop match	0.70385
Brown&Mesa	40–50	No outcrop match	0.70424
Brown&Mesa	100–110	No outcrop match	0.70405
Brown&Mesa	100–110	No outcrop match	0.70428
Brown&Mesa	130–140	No outcrop match	0.70384
Brown&Mesa	130–140	No outcrop match	0.70396
Brown&Mesa	200–210	Verde A	0.70611
Brown&Mesa	200–210	Verde A	0.70593
Brown&Mesa	200–210	Verde B	0.70627
Brown&Mesa	200–210	Verde B	0.70621
Brown&Mesa	200–210	WH	0.70610
Brown&Mesa	340–350	No outcrop match	0.70410
Brown&Mesa	340–350	No outcrop match	0.70312
Brown&Mesa	480–490	No outcrop match	0.70345
Brown&Mesa	480–490	No outcrop match	0.70287
Brown&Mesa	480–490	No outcrop match	0.70275
Brown&Mesa	690–700	No outcrop match	0.70322
Brown&Mesa	690–700	No outcrop match	0.70304
Mesa & Lehi	50–60	No outcrop match	0.70386
Mesa & Lehi	50–60	No outcrop match	0.70432
Mesa & Lehi	90–100	No outcrop match	0.70404
Mesa & Lehi	90–100	No outcrop match	0.70390
Mesa & Lehi	140–150	No outcrop match	0.70408
Mesa & Lehi	140–150	No outcrop match	0.70399
Mesa & Lehi	180–190	WH	0.70610
Mesa & Lehi	180–190	WH	0.70616
Mesa & Lehi	180–190	Verde A	0.70600
Mesa & Lehi	180–190	Verde A	0.70621
Mesa & Lehi	180–190	Verde B	0.70615
Mesa & Lehi	200–210	No outcrop match	0.70305
Mesa & Lehi	200–210	No outcrop match	0.70285
Mesa & Lehi	240–250	No outcrop match	0.70330
Mesa & Lehi	240–250	No outcrop match	0.70283
Mesa & Lehi	240–250	No outcrop match	0.70299
Mesa & Lehi	340–350	No outcrop match	0.70282
Mesa & Lehi	340–350	No outcrop match	0.70302

Mescal Limestone has a distinctive texture when the carbonate dissolves, creating areas of raised relief of the silicified portions (Fig. 7). The results of a clast count revealed that less than 0.1% of the clasts on the terrace surface were Mescal Limestone. With the only known location of a bedrock outcrop being around the location of Roosevelt Dam, the presence of the Mescal Limestone suggests a direct hydrologic connection to the Stewart Mountain Terrace. In other words, the only possible process that could transport these clasts from an outcrop area around Roosevelt Dam to the sampling site would have been by fluvial processes.

We also examined Pliocene fanglomerate in the area of the Stewart Mountain terrace that certainly predates the Salt River, and we have yet to find any definitive Mescal Limestone fragments. This was to test the hypothesis that the Mescal Limestone fragments simply eroded out of the underlying alluvial fan sediment, but we found no evidence of Mescal Limestone in fanglomerate underlying the terrace. Pending future field observations, our tentative conclusion is that the Salt River transported these fragments when it eroded the sill where the river crosses the Mazatzal Mountains.

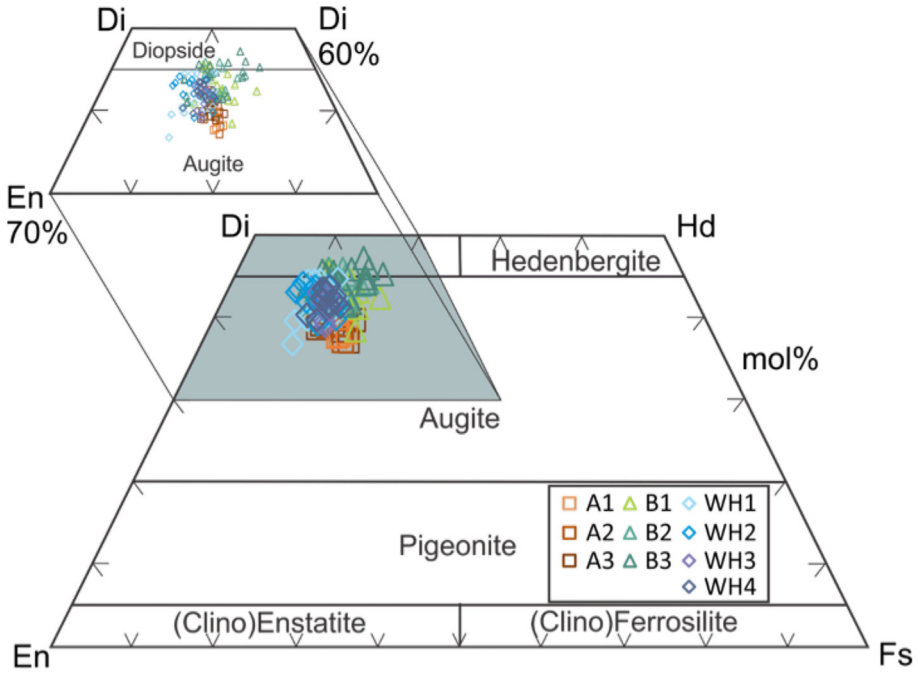

Fig. 12. Pyroxene compositions as molecular ratios of Mg, Fe, and Ca (En-enstatite, Fs-ferrosilite, Hd-hedenbergite, Di-diopside; Morimoto et al., 1988) of the different Verde A (square symbols), Verde B (triangle symbols), and Wildhorse (diamond symbols) samples cluster together. Samples A1 and B1 refer to outcrop samples at Verde A, B (Fig. 2). Samples A2 and B2 refer to clasts collected from the base of the Lousley Hills gravels (Fig. 6), Samples A3 and B3 refer to clasts collected from the well cuttings (Fig. 8). Samples WH1 and WH2 refer to clasts collected from outcrop samples, whereas WH3 and WH4 are from well cuttings. The insert shows greater detail of the dark gray region.

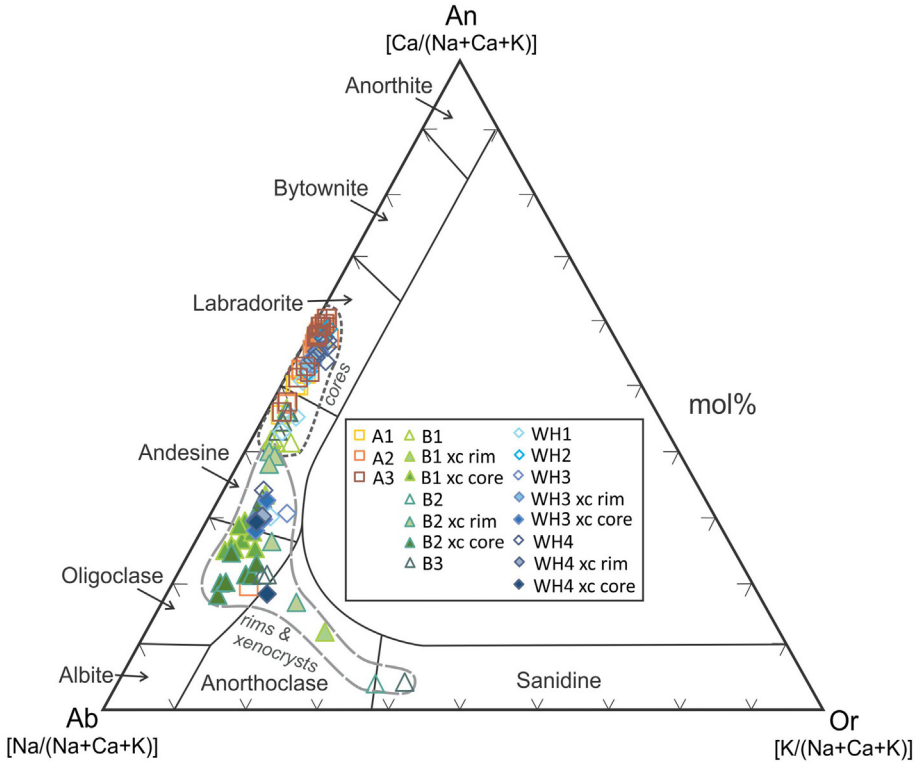

Fig. 13. Plagioclase compositions of Verde A (square symbols), Verde B (triangle symbols), and Wildhorse (diamond symbols) samples clustered together. "xc" means xenocryst; xenocrystic plagioclase occurs in samples Verde B2, Verde B3, WH3, and WH4. Plagioclase crystals are zoned with K-enriched rims. Compositions of Verde A and WH plagioclase (labradorite) are indistinguishable, whereas B-plagioclase tends towards andesine compositions. Samples A1 and B1 refers to outcrop samples at Verde A, B (Fig. 2). Samples A2 and B2 refer to clasts collected from the base of the Lousley Hills gravels (Fig. 6), Samples A3 and B3 refer to clasts collected from the well cuttings (Fig. 8). Samples WH1 and WH2 refer to clasts collected from outcrop samples, whereas WH3 and WH4 are from well cuttings. Rim refers to the outer margins of the clasts in Fig. 4, whereas core refers to the inside of the clasts in Fig. 4.

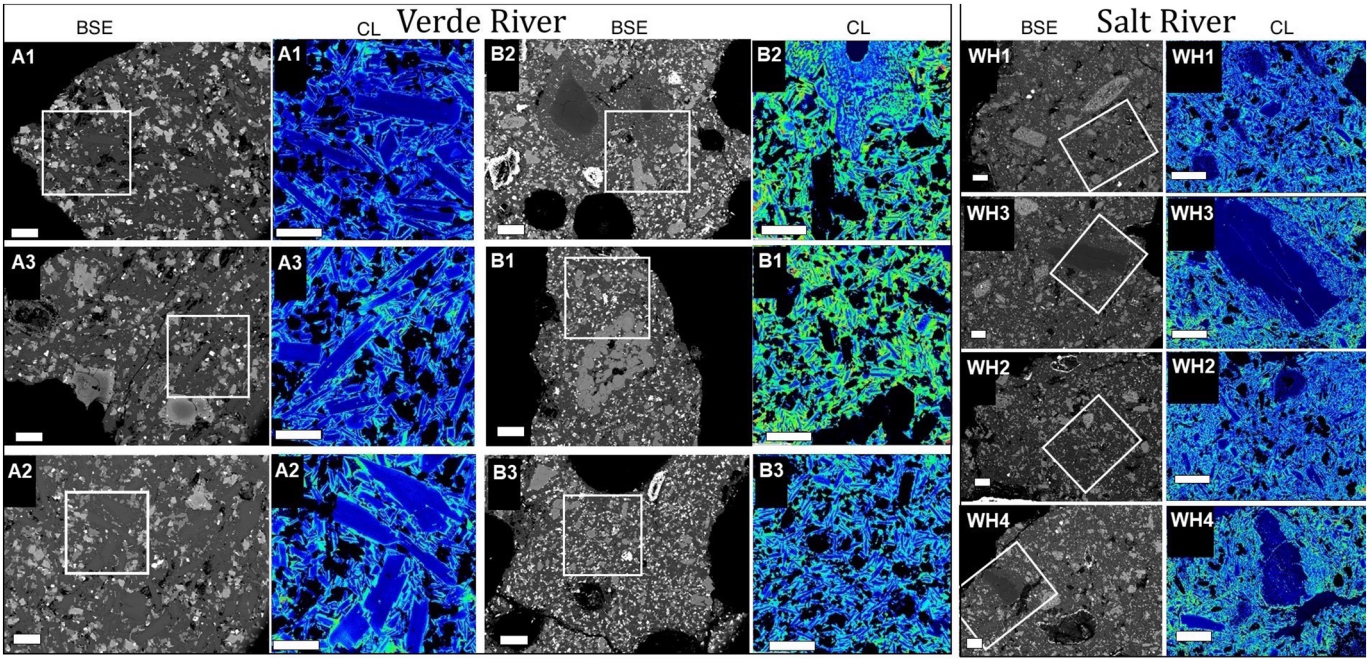

Fig. 14. Representative cathodoluminescence images (CL) and correlated back-scattered electron (BSE) images of basalt clasts taken from the base of the ASRD in the Mesa and Lehi well (A2, B3, WH2, WH4; Fig. 8), the Lousley Hills stream terrace of the Verde River (A3, B1; Fig. 4), and then the identified potential sources at the outcrop sites of Verde A and B (A1, B2, WH1, WH3). Our interpretation is that a visual analysis of these textures does not reveal any significant differences between source and basalt materials removed from the base of the ASRD. The scale bars on all images are 200 μm. The boxes on the BSE images indicate the locations of the cathodoluminescence images. The samples displayed in Fig. 4 are those presented in this figure, where the different numbers of associated with Verde A, Verde B, and Wildhorse samples are internal notations to different subsample frames.

5. Discussion

Rivers cross mountains or structural highs using four different mechanisms (Douglass and Schmeeckle, 2007; Douglass et al., 2009). (i) Rivers can predate the uplift and incise into the mountain as it rises (antecedence) or (ii) can be laid down upon a structural high from an eroding covermass (superimposition). Other rivers postdate the uplift and (iii) form via piracy, including headward erosion of streams that capture an upstream drainage area, or (iv) they may integrate through downward "top down" progression via lake overflow.

The presence of the 3.3 Ma Nomlaki tuff (Table 1; Fig. 2A) intercalated with the Pemberton Ranch playa deposits (Skotnicki et al., 2003) means that neither antecedence nor superimposition can explain integration of the Salt or the Verde rivers; the reason is that the Pemberton Ranch playa started to erode when the two rivers integrated sometime after 3.3 Ma. The tectonic basins and mountainous terrain between the high areas of these drainage systems developed as a result of Neogene extension more than ten million years before 3.3 Ma (Anderson and Piety, 1988; Scarborough, 1989; Spencer and Reynolds, 1989; Houser, 1990). A river that post-dates a structural high can only form through either piracy or lake overflow (Douglass et al., 2009).

Skotnicki and DePonty (2020) analyzed the rock types found in different wells that record basin fill and then the ancestral Salt River deposits (ASRD). Skotnicki et al. (in this issue) concluded that the lithology found in Pliocene alluvial fan deposits in the lower Verde River valley (Fig. 2A) called "The Rolls" formation were a match for basin fill far underneath the ASRD. In preserved outcrops. The Rolls fanglomerate contain clasts that originate in the Mazatzal Mountains. These materials were able to reach the East Salt River (Higley) basin (Fig. 3) when the lower Verde River valley existed in a state of overspill (as portrayed in Fig. 2A). Skotnicki et al. (in this issue) postulate that this overspill condition existed for much of the Pliocene. Thus, when The Rolls alluvial fan spilled over into the Higley basin, the basin-fill sediment would have mixed with sources of sediment from the Higley basin and the upstream lower Verde River basin.

Because The Rolls Formation formed a "ramp" of alluvial-fan material from the lower Verde River valley to reach into the Higley basin (Skotnicki et al., this issue), the detrital zircon (DZ) analyses of the basin fill (Figs. 9 and 10) should have some small degree of similarity to DZ analyses of the ASRD. The reason can be seen in Fig. 2A and B, where the integrated Salt River drainage (Fig. 2B) includes the lower Verde River valley between the McDowell and Mazatal mountains (Fig. 2A).

The clear finding of the DZ results presented in Figs. 9 and 10 reveal that basin-fill deposits contain different and distinct sources of sediment than the ancestral Salt River deposits because probability peaks do not match well. These results confirm the original interpretation of Laney and Hahn (1986) and the mineralogical logs of Skotnicki and DePonty (2020) that the Salt River arrived suddenly in the Phoenix's East Salt River (Higley) basin.

However, basin-fill peaks and the ASRD peaks do have some similarities to the basin fill: (i) smaller basin-fill peaks at 19 Ma, 1200 Ma, 1450 Ma, 1750 Ma, and 1850 Ma; and (ii) similar sized peaks at 21 Ma, 1050 Ma, 1300 Ma and 1500 Ma. For example, the 19 Ma Neogene explosive Superstition volcanic material shed into the Rolls Formation and also into the Salt River. Thus, the DZ results are consistent with the idea that the Rolls Formation material underneath the ASRD (Skotnicki et al., in this issue) contributed sediment into the early Salt River deposit.

Additional DZ analyses from different depths in the ASRD could reveal important insights. Consider a newly-arrived Salt River flowing on the hypothesized alluvial-fan ramp of The Rolls formation (Skotnicki et al., in this issue). This initial discharge would be "mining" the loose sediment of The Rolls formation and could represent the initial ASRD deposits. Then, as a knickpoint eroded back into the Tonto Basin (Fig. 2B), the composition of the ASRD would be expected to contain a lower and lower percentage of lower Verde River valley sediment. Thus, the ~170 ft (52 m) depth of the DZ deposit in the Brown and Mesa Dr. well (Fig. 8A) could reflect this transition in a source region for ASRD materials.

Provenance analyses of basalts using trace elements, electron microprobe measurements of pyroxene and plagioclase minerals, electron

microscopy CL and BSE imagery, and $^{87}Sr/^{86}Sr$ analyses of basalt cobbles collected from the base of the ASRD (Fig. 8) place outcrop sources in the lower Verde River drainage and the lower Salt River drainage. Because basalt clasts from these two different drainages arrived at the same depth in two different well locations, it is not possible to determine which river integrated first – the Salt River or the Verde River. To the limits of sampling resolution of 3 m intervals in the two wells (Fig. 8), two different drainages appeared to have supplied sediment to the base of the ASRD in the same time period.

Larson et al. (2010) identified the Stewart Mountain Terrace (Fig. 7A) as the highest possible terrace of the Salt River and interpreted it to be a fill terrace. Skotnicki et al. (in this issue) recognized that the much of material underlying the terrace surface was Rolls Formation and not Salt River in origin. The presence of the Mescal Limestone gravels scattered across the surface (Fig. 7B), however, indicates that this high topographic surface is a strath terrace. If the Salt River integrated across the Mazatzal Mountains via lake overflow as postulated by Douglass et al. (2009), it would have first sent relatively clean water down the lowest topography that would have been the location of the Rolls Formation alluvial fan. Then, knickpoint retreat after lake water overtops the sill (Douglass and Schmeeckle, 2007; Douglass et al., 2009) would have eroded the Mescal Limestone that is prevalent around the sill (Fig. 7A). Dickinson's (2015) headward erosion hypothesis neither explains the presence of the Stewart Mountain Terrace, nor why Mescal Limestone clasts should be present in this high terrace, but not in any of the lower Salt River terraces (Kokalis, 1971; Péwé, 1978).

The basalt provenance analyses (Figs. 11–14; Table 2) cannot be explained by the Salt and Verde rivers eroding headward to get across mountain barriers located at the present-day positions of Stewart Mountain Dam and Bartlett Dam. Headward extension of any given drainage works at different timescales (Crosby and Whipple, 2006; Darling and Whipple, 2015), and there is no reason to think the pace of headward erosion of an ancestral Salt or Verde river system would reach outcrop deposits at the same time. If these rivers extended via headward erosion, the basalt deposits should have been eroded at very different times. Thus, the penecontemporaneous arrival of basalt clasts from two different drainage systems would be a ridiculously unlikely event from headward extension. Furthermore, there is no evidence of these outcrop basalt clasts in the basin fill underneath the ASRD, and yet rivers extending headward into the Verde A,B and WH locations (Fig. 2) should send material from these locations to the basin fill. However, no basalts extracted from the basin fill match the aforementioned outcrops. Not finding any matches between the WH, Verde A, or Verde B outcrops above the basal layers of the ASRD would be consistent with rivers adjusting their longitudinal profiles and incising beneath these outcrops.

Lake overflow of the Verde over the structural high occupied by Bartlett Dam and also of the Salt River over the structural high occupied by Roosevelt Dam would explain all of the evidence presented in this paper. First, the Pemberton Ranch playa deposit (Skotnicki et al., 2003) existed in a closed basin (Fig. 2) until after 3.3 Ma, and overflow would have led to erosion of the playa sediment. Second, overflow would have eroded the basalt outcrops in the Verde and Salt rivers because the first stage of lake overflow is relatively clean water that flows over a sill. The basalt would have then been transported to the lowest point in the region — the Higley Basin (or the East Salt River Basin) at the present-day location of Mesa, Arizona (Nations et al., 1982; Peirce, 1984; Spencer et al., 2001). This transportation event resulted in the deposition of the ASRD.

Furthermore, the process of lake overflow is compatible with known timing for major drainage integration events in the central Arizona region. Magnetostratigraphy studies of lake sediment in the present-day location of the Verde River valley at Cottonwood, Arizona, indicate that this upstream lake stopped depositing sediment ca. 2.5 Ma (Bressler and Butler, 1978). Because river integration from lake overflow tends to be a top-down series of events breaching progressively lower basins (Spencer and Pearthree, 2001; House et al., 2008; Roskowski et al., 2010; Repasch et al., 2017), the existence of the Nomlaki tuff in closed-basin playa sediment (Table 1) at 3.3 Ma would be consistent with an upstream breaching event at 2.5 Ma.

The trace element (Supplemental File 1) and Sr-isotope results (Table 2) from basalt clasts collected under the Gillespie shield volcano at Cave's (2015) S-06-180c field site are consistent with basalt clasts originating from the Verde B outcrop (Table 2). Our preliminary interpretation, that needs to be tested with further analyses of other basalt clasts underneath Sentinel Volcanic Field basalt flows (Cave, 2015), is that the Verde River contributed alluvium to this location earlier than 2.3 Ma. These initial findings are consistent with the likely start of a through-flowing Verde River at about 2.5 Ma (Pearthree, 1993).

If the Verde River originated by headward erosion up into the lake where the Verde Formation ceased depositing ca. 2.5 Ma (Bressler and Butler, 1978), it would have to have first crossed the structural high near modern-day Bartlett Dam and done so after 3.3 Ma when the Nomlaki tuff was deposited in playa sediment (Fig. 2; Table 1). Then, a headward extending Verde River would have to have taken <0.8 Ma to cross several mountainous transverse drainage sections over a distance of 97 km at a rate > 12 cm/yr. Such rapid rates of headward erosion are inconsistent with numerical modeling studies (Geurts et al., 2018, 2020). Although this rapid rate of knickpoint retreat occurs in situations like Niagara Falls, rates of >12 cm/yr are extraordinary (Loget and Van Den Driessche, 2009a, 2009b). The burden would rest on proponents of headward extension to provide clear evidence that a headward-eroding stream working in topography like Arizona's Transition Zone would be capable of this anomalous rate.

6. Conclusion

The Salt River and Verde River drainages supply much of the water to metropolitan Phoenix, Arizona, USA. Yet, these rivers did not exist as through-flowing streams at 3.3 Ma when the Nomlaki tuff fell onto a closed-basin playa located at the modern-day junction of these two major rivers. This paper provides new insight into how the Salt and Verde rivers integrated across mountainous barriers.

Out of the four possible processes to explain drainage integration — antecedence, superimposition, piracy, and lake overflow — only lake overflow is not contradicted by the research presented here. Because the age of the structural basins and intervening mountains are much older (Anderson and Piety, 1988; Scarborough, 1989; Spencer and Reynolds, 1989; Houser, 1990) than origin of the Salt and Verde rivers after 3.3 Ma, neither antecedence nor superimposition can explain the creation of these exoreic rivers. Both of these processes require the river to be older than the structural highs that it crosses (Douglass et al., 2009). Rivers like the Salt and Verde that post-date the formation of a structural high can only form through either piracy or lake overflow (Douglass et al., 2009).

Samples for detrital zircons (DZ) and basalt analysis were removed from cuttings of two wells in Mesa, Arizona, located in the East Salt River (or Higley) structural basin in the Basin and Range Province of western North America. These well cuttings reveal a sudden transition from basin-fill deposits to ancestral Salt River deposits (ASRD) (Skotnicki and DePonty, 2020). Detrital zircon analyses from the basin-fill sediment and the overlying ancestral Salt River deposits (ASRD) reveal notable differences, confirming the original interpretation of Laney and Hahn (1986) and the mineralogic logs (Skotnicki and DePonty, 2020) that the ASRD represents the sudden onset of drainage integration.

Drainage piracy by the process of headward-eroding streams rests in conflict with several types of evidence presented in this research. Basalt cobbles were removed from well cuttings from multiple depths in the basin fill and ASRD. Some basalt clasts at the base of the ASRD have properties that match very closely with outcrop locations in the lower Verde and lower Salt River drainages. The matching provenance properties include trace element, $^{87}Sr/^{86}Sr$ ratios, major and minor element chemistries of pyroxene and plagioclase grains, cathodoluminescence

textures, and back-scattered electron microscope textures. Basalt clasts from the basin fill below and the ASRD sediments above the first arriving Salt River sediments do not match outcrop basalts.

One implication of the basalt clast provenance research presented here is that the position of the Salt and Verde rivers shifted away from these outcrop positions soon after drainage integration. In the case of the Verde River, its position shifted to the east, and the Salt River shifted to the north over time. Another implication of the basalt clast study is that piracy through headward erosion likely did not integrate the Salt or Verde rivers. Headward erosion would have transported the basalt clasts prior to drainage integration and deposited them in the basin fill — and there is no evidence of this. Headward erosion would proceed at a different pace in different river systems, and yet clasts from the Verde and Salt drainages arrived at a similar time to deposit in the base of the ASRD. Thus, we conclude that the best interpretation is that both the Salt and Verde rivers integrated by the process of lake overflow.

Another finding of this study in conflict with headward erosion establishing the Salt River comes from a study of the provenance of Mescal Limestone clasts found on the surface of the Stewart Mountain terrace, whose only source is at the sill where the Salt River flows across the Mazatzal Mountains separating the Tonto Basin from lower basins. Integration by lake overflow near modern-day Roosevelt Dam would have led to knickpoint retreat and erosion of the Mescal Limestone clasts that were then transported to the then-low spot — now occupied by the Stewart Mountain Terrace. Ongoing longitudinal profile adjustments led to floodplain abandonment, leaving behind Mescal Limestone clasts on this strath terrace. However, headward erosion back up into the Mazatzal Mountains would have led to a longer longitudinal profile and gradual incision of a river into the pre-existing topography (Larson et al., 2010). Headward erosion would not explain why Mescal Limestone clasts are present on this high terrace, and not in any of the lower Salt River terraces (Kokalis, 1971; Péwé, 1978).

Integration of the Salt and Verde rivers via lake overflow is compatible with evidence presented here on the timing of drainage integration. Furthermore, our provenance evidence is compatible with results of the established method of using geomorphic criteria to adjudicate between different drainage integration processes, an approach indicating Salt River drainage integration via lake overflow (Douglass et al., 2009).

Magnetostratigraphy studies of Verde Formation deposits indicate that a major lake upstream of the study area stopped depositing ca. 2.5 Ma (Bressler and Butler, 1978), leading to a through-flowing Verde River (Pearthree, 1993) and destruction of the playa sometime after when the Nomlaki tuff accumulated closed-basin playa sediment (Table 1) at 3.3 Ma. In contrast, if the Verde River originated by headward extension, an exceptionally fast rate of headward extension of over 12 cm/yr across multiple bedrock features would demand clear evidence of processes that could produce such an extraordinary rate (Loget and Van Den Driessche, 2009a, 2009b) in under 800,000 yr.

Supplementary data to this article can be found online at https://doi.org/10.1016/j.geomorph.2020.107430.

Declaration of competing interest

The authors declare that they have no known competing financial interests or personal relationships that could have appeared to influence the work reported in this paper.

Acknowledgements

We thank Brian F. Gootee, Emily Zawacki, Philip A. Pearthree, Zach Hilgendorf, and Scott Lecce for comments that greatly improved the paper, Salt River Project (Modification 35 to Cooperative Agreement 98-153C) for partial support of this research, Arial Shamas and Alexis Ruiz for the scientific illustration in Fig. 2 and the graphical abstract, and Michelle Aigner for help in the detrital zircon analyses.

References

Anderson, L., Piety, L.A. (Eds.), 1988. Field-Trip Guidebook to the Tonto Basin: Geomorphology, Quaternary Geology, Tertiary Basin Development, Archaeology, and Engineering Geology: Friends of the Pleistocene. Rocky Mountain Cell of the Friends of the Pleistocene. 186 p., 1 sheet, scale 1: 48,000.

Bilodeau, W.L., 1986. The Mesozoic Mogollon Highlands, Arizona: an early cretaceous rift shoulder. The Journal of Geology 94, 724–735.

Bressler, S.L., Butler, R.F., 1978. Magnetostratigraphy of the late Tertiary Verde Formation, central Arizona. Earth Planet. Sci. Lett. 38, 319–330.

Brokus, S.A., Silletti, D.K., Lunderberg, J.M., DeYoung, P.A., Carpenter, D.E., Buscaglia, J., 2015. Cathodoluminescence dependence on feldspar mineral structure and implications for forensic geology. Am. Mineral. 100, 451–458.

Cave, S.R., 2015. The Sentinel-Arlington Volcanic Field, Arizona. Ph.D. Dissertation, Arizona State University, Tempe, 59 p.

Cave, S., Greeley, R., 2004. The geology of two small Cenozoic Volcanoes in Southwestern Arizona. J. Ariz. Nev. Acad. Sci. 37, 105–110.

Collins, A.L., Walling, D.E., Leeks, G.J., 1997. Fingerprinting the origin of fluvial suspended sediment in larger river basins: combining assessment of spatial provenance and source type. Geografiska Annaler: Series A, Physical Geography 79, 239–254.

Connell, S.D., Hawley, J.W., Love, D.W., 2005. Late Cenozoic drainage development in the southeastern Basin and Range of New Mexico, Southeasternmost Arizona, and western Texas. New Mexico Museum of Natural History and Science Bulletin 28, 125–150.

Craddock, W.H., Kirby, E., Harkins, N.W., Zhang, H., Shi, X., Liu, J., 2010. Rapid fluvial incision along the Yellow River during headward basin integration. Nat. Geosci. 3, 209–213.

Crosby, B.T., Whipple, K.X., 2006. Knickpoint initiation and distribution within fluvial networks: 236 waterfalls in the Waipaoa River, North Island, New Zealand. Geomorphology 82, 16–38.

Darling, A., Whipple, K., 2015. Geomorphic constraints on the age of the western Grand Canyon. Geosphere 11, 958–976.

Dethier, D.P., 2001. Pleistocene incision rates in the western United Stated calibrated using Lava Creek B tephra. Geology 29, 783–786.

Dickinson, W.R., 2015. Integration of the Gila River drainage system through the Basin and Range province of southern Arizona and southwestern New Mexico (USA). Geomorphology 236, 1–24.

Douglass, J., Schmeeckle, M.W., 2007. Analogue modeling of transverse drainage mechanisms. Geomorphology 84, 22–43.

Douglass, J., Meek, N., Dorn, R.I., Schmeeckle, M.W., 2009. A criteria-based methodology for determining the mechanism of transverse drainage development, with application to southwestern USA. Geol. Soc. Am. Bull. 121, 586–598.

Fertelmes, C., Glascock, M.D., 2018. Destructive and nondestructive geochemical analysis of vesicular basalt from bedrock outcrops in the Salt-Gila Basin, Arizona: evaluating the potential of nondestructive portable X-ray fluorescence spectroscopy for archaeological provenance analyses. J. Archaeol. Sci. Rep. 19, 769–780.

Fitzgerald, P.G., Reynolds, S.J., Stump, E., Foster, D.A., Gleadow, A.J.W., 1993. Thermochronologic evidence for timing of denudation and rate of crustal extension of the South Mountains metamorphic core complex and Sierra Estrella, Arizona. Nuclear Tracks and Radiation Measurements 21, 555–563.

Geurts, A.H., Cowie, P.A., Duclaux, G., Gawthorpe, R.L., Huismans, R.S., Pedersen, V.K., Wedmore, L.N., 2018. Drainage integration and sediment dispersal in active continental rifts: a numerical modelling study of the central Italian Apennines. Basin Res. 30, 965–989.

Geurts, A.H., Whittaker, A.C., Gawthorpe, R.L., Cowie, P.A., 2020. Transient landscape and stratigraphic responses to drainage integration in the actively extending central Italian Apennines. Geomorphology 353, 107013. https://doi.org/10.1016/j.geomorph.2019.107013.

Gilbert, G.K., 1928. Studies of basin-range structure. U.S. Geol. Surv. Prof. Pap. 153, 1–92.

Gluhak, T.M., Rosenberg, D., 2018. Back to the Source—Geochemical Data from Israel for the provenance analyses of basaltic rock artefacts and their implications on previous and future studies. Archaeometry 60, 1153–1169.

House, P.K., Pearthree, P.A., Perkins, M.E., 2008. Stratigraphic evidence for the role of lake spillover in the inception of the lower Colorado River in southern Nevada and western Arizona. Geol. Soc. Am. Spec. Pap. 439, 335–353.

Houser, B.B., 1990. Late Cenozoic strateigrpahy and tectonics of the Safford basin, southeastern Arizona. In: Gehrels, G.E., Spencer, J.E. (Eds.), Geologic Excursions Through the Sonoran Desert Region, Arizona and Sonora. Arizona Geological Survey Special Paper. vol. 7. Arizona Geological Survey, Tucson, pp. 20–24.

Howard, K.A., House, P.K., Dorsey, R.J., Pearthree, P.A., 2015. River-evolution and tectonic implications of a major Pliocene aggradation on the lower Colorado River: the Bullhead Alluvium. Geosphere 11, 1–30.

Izett, G.A., Wilcox, R.E., 1982. Map Showing Localities and Inferred Distributions of the Huckleberry Ridge, Mesa Falls, and Lava Creek Ash Beds (Pearlette Family Ash Beds) of Pliocene and Pleistocene Age in the Western United States and Southern Canada. U.S. Geological Survey Miscellaneous Investigations Series Map 1325. https://ngmdb.usgs.gov/Prodesc/proddesc_9153.htm.

Jungers, M.C., Heimsath, A.M., 2016. Post-tectonic landscape evolution of a coupled basin and range: Pinaleño Mountains and Safford Basin, southeastern Arizona. Geol. Soc. Am. Bull. 128 (469–486).

Jungers, M.C., Heimsath, A.M., 2019. Transverse canyon incision and sedimentary basin excavation driven by drainage integration, Aravaipa Creek, AZ, USA. Earth Surface Processes and Landforms https://doi.org/10.1002/esp.4556 in press.

Kimbrough, D.L., Grove, M., Gehrels, G.E., Dorsey, R.J., Howard, K.A., Lovera, O., Aslan, A., House, P.K., Pearthree, P.A., 2015. Detrital zircon U-Pb provenance record of the Colorado River: implications for late Cenozoic drainage evolution of the American Southwest. Geosphere 11, 1–30.

Kokalis, P.G., 1971. Terraces of the Lower Salt River Valley. ArizonaMasters, Arizona State University, Tempe 103 pp.
Krinsley, D.H., Pye, K., Boggs, S., Tovey, K.K., 2005. Backscattered Electron Microscopy and Image Analysis of Sediments and Sedimentary Rocks. Cambridge University Press, Cambridge, U.K.
Labrenz, M.E., Karlstrom, K.E., 1991. Timing of the Mazatzal orogeny: Constraints from the Young Granite, Pleasant Valley, Arizona. Arizona Geological Society Digest 19, 225–236.
Laney, R.L., Hahn, M.E., 1986. Hydrogeology of the eastern part of the Salt River Valley area, Maricopa and Pinal Counties, Arizona. U.S. Geological Survey Water-resources Investigations Report 86-4147, 4 plates.
Larson, P.H., Dorn, R.I., Douglass, J., Gootee, B.F., Arrowsmith, R., 2010. Stewart Mountain Terrace: a new Salt River terrace with implications for landscape evolution of the lower Salt River Valley, Arizona. J. Ariz. Nev. Acad. Sci. 42, 26–36.
Leeman, W.P., 1970. The isotopic composition of strontium in late-Cenozoic basalts from the Basin-Range province, western United States. Geochim. Cosmochim. Acta 34, 857–872.
Leeman, W.P., 1982. Tectonic and magmatic significance of strontium isotopic variations in Cenozoic volcanic rocks from the western United States. Geol. Soc. Am. Bull. 93, 487–503.
Leier, A.L., Gehrels, G.E., 2011. Continental-scale detrital zircon provenance signatures in Lower Cretaceous strata, western North America. Geology 39, 399–402.
Linthout, K., 2015. Provenance of the Roman basalt stone at Kotterbos (Lelystad, the Netherlands): a geoarchaeological study based on petrographic and geochemical analysis, and comparison with a synthesis of basalt stones along the northern Limes. Netherlands Journal of Geosciences 94. https://doi.org/10.1017/njg.2014.45.
Loget, N. and Van Den Driessche, J., 2009a. Wave train model for knickpoint migration. Geomorphology106, 376–382.
Loget, N., Van Den Driessche, J., 2009b. Wave train model for knickpoint migration. Geomorphology 106, 376–382.
Malusà, M.G., Wang, J., Garzanti, E., Liu, Z.C., Villa, I.M., Wittmann, H., 2017. Trace-element and Nd-isotope systematics in detrital apatite of the Po river catchment: implications for provenance discrimination and the lag-time approach to detrital thermochronology. Lithosphere 290, 48–59.
McAlister, A., Allen, M.S., 2017. Basalt geochemistry reveals high frequency of prehistoric tool exchange in low hierarchy Marquesas Islands (Polynesia). PLoS One 12 (12), e0188207.
McGee, L.E., Smith, I.E., 2016. Interpreting chemical compositions of small scale basaltic systems: a review. J. Volcanol. Geotherm. Res. 325, 45–60.
McIntosh, W.C., Ferguson, C.A., 1998. Sanidine, single crystal, laser-fusion 40Ar/39Ar geochronology database for the Superstition volcanic field, central Arizona. Arizona Geological Survey Open File Report 98-27, 1–74.
Meek, N., 1989. Geomorphic and hydrologic implications of the rapid incision of Afton Canyon, Mojave Desert, California. Geology 17, 7–10.
Meek, N., 2004. Mojave River history from an upstream perspective. In: Reynolds, R.E. (Ed.), Breaking up — the 2004 Desert Symposium Field Trip and Abstracts. California State University Fullerton Desert Studies Consortium, Fullerton, CA, pp. 41–49.
Meek, N., 2019. Episodic forward prolongation of trunk channels in the Western United States. Geomorphology 340, 172–183. https://doi.org/10.1016/j.geomorph.2019.05.002.
Melton, M.A., 1965. The geomorphic and paleoclimatic significance of alluvial deposits in southern Arizona. J. Geol. 73, 1–38.
Morgan, L.A., McIntosh, W.C., 2005. Timing and development of the Heise volcanic field, Snake River Plain, Idaho, western USA. Geol. Soc. Am. Bull. 117, 288–306.
Morimoto, N., Fabries, J., Ferguson, A.K., Ginzburg, I.V., Ross, M., Seifert, F.A., Zussman, J., Aoki, K., Gottardi, G., 1988. Nomenclature of pyroxenes. Am. Mineral. 73, 1123–1133.
Mounteney, I., Burton, A.K., Farrant, A.R., Watts, M.J., Kemp, S.J., Cook, J.M., 2018. Heavy mineral analysis by ICP-AES a tool to aid sediment provenancing. J. Geochem. Explor. 184, 1–10.
Nations, J.D., Landye, J.J., Hevly, R.H., 1982. Location and chronology of the Tertiary sedimentary deposits in Arizona: a review. In: Ingersoll, R.V., Woodburne, M.O. (Eds.), Cenozoic Non Marine Deposits of California and Arizona. Society for Sedimentary Geology, Broken Arrow, OK, pp. 107–122.
Óladóttir, B.A., Sigmarsson, O., Larsen, G., Devidal, J.L., 2011. Provenance of basaltic tephra from Vatnajökull subglacial volcanoes, Iceland, as determined by major-and trace-element analyses. The Holocene 21, 1037–1048.
Pearthree, P.A., 1993. Geologic and geomorphic setting of the Verde River from Sullivan Lake to Horseshoe Reservoir. Arizona Geological Survey Open File Report 93-4, 1–27.
Pearthree, P.A., House, P.K., 2014. Paleogeomorphology and evolution of the early Colorado River inferred from relationships in Mohave and Cottonwood valleys, Arizona, California, and Nevada. Geosphere 10, 1139–1160.
Peirce, H.W., 1984. Some late Cenozoic basins and basin deposits of southern and western Arizona. In: Smiley, T.L., Nations, J.D., Péwé, T.L., Schafer, J.P. (Eds.), Landscapes of Arizona. University Press of America, Tucson, pp. 207–227.
Péwé, T.L., 1978. Guidebook to the Geology of Central Arizona. Arizona Bureau of Geology and Mineral Technology Special Paper 2.
Poletski, S.J., 2010. The Nomlaki Tuff eruption: Chemical correlation of a widespread Plicoene stratigraphic marker. M.S. Thesis, Geology. California State University, Sacramento.
Repasch, M., Karlstrom, K., Heizler, M., Pecha, M., 2017. Birth and evolution of the Rio Grande fluvial system in the past 8 Ma: progressive downward integration and the influence of tectonics, volcanism, and climate. Earth Sci. Rev. 168, 113–164.
Richard, S.M., Shipman, T.C., Greene, L., Harris, R. C., 2007. Estimated depth to bedrock in Arizona. Arizona Geological Survey Digital Geologic Map 52, 1-1.
Rosenberg, D., Shimelmitz, R., Gluhak, T.M., Assaf, A., 2015. The geochemistry of basalt handaxes from the Lower Palaeolithic site of Ma'ayan Baruch, Israel—a perspective on raw material selection. Archaeometry 57 (S1), 1–19.
Roskowski, J.A., Patchett, P.J., Spencer, J.E., Pearthree, P.A., Dettman, D.L., Faulds, J.E., Reynolds, A.C., 2010. A late Miocene–early Pliocene chain of lakes fed by the Colorado River: evidence from Sr, C, and O isotopes of the Bouse Formation and related units between Grand Canyon and the Gulf of California. Geol. Soc. Am. Bull. 122, 1625–1636.
Sarna-Wojcicki, A.M., Reheis, M.C., Pringle, M.S., Fleck, R.J., Burbank, D., Meyer, C.E., Slate, J. L., Wan, E., Budahn, J.R., Troxel, B., Walker, J.P., 2005. Tephra layers of Blind Spring Valley and related upper Pliocene and Pleistocene tephra layers, California, Nevada, and Utah: Isotopic ages, correlation, and magnetostratigraphy. U.S. Geol. Surv. Prof. Pap. 1701, 1–69.
Sarna-Wojcicki, A.M., Deino, A.L., Fleck, R.J., McLaughlin, R.J., Wagner, D., Wan, E., Wahl, D., Hillhouse, J.W., Perkins, M., 2011. Age, composition, and areal distribution of the Pliocene Lawlor Tuff, and three younger Pliocene tuffs, California and Nevada. Geosphere 7, 599–628.
Scarborough, R.B., 1989. Cenozoic erosion and sedimentation in Arizona. Arizona Geological Society Digest 17, 515–537.
Scholonek, C., Augustsson, C., 2016. Can cathodoluminescence of feldspar be used as provenance indicator? Sediment. Geol. 336, 36–45.
Shafiqullah, M., Damon, P.E., Lynch, D.J., Reynolds, S.J., Rehrig, W.A., Raymond, R.H., 1980. K-Ar geochronology and geologic history of southwestern Arizona and adjacent areas. Arizona Geological Society Digest 12, 201–260.
Skotnicki, S.J., 1996. Geologic Map of the Bartlett Dam Quadrangle and southern part of the Horseshoe Dam Quadrangle, Maricopa County, Arizona. Arizona Geological Survey Open File Report 96-22, 1–22.
Skotnicki, S.J., 2000. Geologic Map of the Four Peaks 7.5′ Quadrangle, Maricopa and Gila Counties, Arizona. Arizona Geological Survey Open-File Report OFR-00-11, 1 map sheet, map scale 1:24,000, 001–035.
Skotnicki, S.J., DePonty, J., 2020. Subsurface evidence for the sudden integration of the Salt River across the internally drained Basin and Range Province, Arizona, USA. Geomorphology, 107429 https://doi.org/10.1016/j.geomorph.2020.107429.
Skotnicki, S.J., Ferguson, C.E., 1996. Bedrock geologic map of the Apache Junction and Buckhorn quadrangles, Maricopa and Pinal Counties, Arizona. Arizona Geological Survey Open-File Report 96-8, 1–16.
Skotnicki, S.J., Young, E.M., Goode, T.C., Bushner, T.C., 2003. Subsurface geologic investigation of Fountain Hills and the Lower Verde River Valley, Maricopa County, Arizona. Arizona Geological Survey Contributed Report CR-03-B, 1–44.
Skotnicki, S.J., Seong, Y.B., Dorn, R., Larson, P.H., DePonty, J., 2020. Drainage integration of the Salt and Verde Rivers in a basin and range extensional landscape, central Arizona, USA. Geomorphology this issue.
Sonder, L.J., Jones, C.H., 1999. Western United States extension: how the west was widened. Annual Reviews of Earth and Planetary Sciences 27, 417–462.
Spencer, J.E., Pearthree, P.A., 2001. Headward erosion versus closed basin spillover as alternative causes of neogene capture of the ancestral Colorado River by the Gulf of California. In: Young, R.A., Spamer, E.E. (Eds.), Colorado River Origin and Evolution: Grand Canyon. Grand Canyon Association, Grand Canyon, pp. 215–219.
Spencer, J.E., Reynolds, S.J., 1989. Middle Tertiary tectonics of Arizona and adjacent areas. Arizona Geological Society Digest 17, 539–574.
Spencer, J.E., Richard, S.M., 1999. Geologic map and report for the Theodore Roosevelt Dam area, Gila and Maricopa Counties, Arizona. Arizona Geological Survey Open File Report 99-6, 1–30.
Spencer, J.E., Richard, S.M., Ferguson, C.A., 2001. Cenozoic structure and evolution of the boundary between the Basin and Range and Transition Zone provinces in Arizona. In: Erskine, M.C., Faulds, J.E., Bartley, J.M., Rowley, P.D. (Eds.), The Geologic Transition, High Plateaus to Great Basin - a Symposium and Field Guide (the Mackin Volume). Utah Geological Association, Salt Lake City, pp. 273–289.
Spencer, J.E., Patchett, P.J., Pearthree, P.A., House, P.K., Sarna-Wojcicki, A.M., Wan, E., Roskowski, J.A., Faulds, J.E., 2013. Review and analysis of the age and origin of the Pliocene Bouse Formation, lower Colorado River Valley, southwestern USA. Geosphere 9. https://doi.org/10.1130/GES00896.00891.
Stewart, J.H., Gehrels, G.E., Barth, A.P., Link, P.K., Christie-Blick, N., Wrucke, C.T., 2001. Detrital zircon provenance of Mesoproterozoic to Cambrian arenites in the western United States and northwestern Mexico. Geol. Soc. Am. Bull. 113, 1343–1356.
Talbot, M.R., Williams, M.A.J., Adamson, D.A., 2000. Strontium isotope evidence for late Pleistocene reestablishment of an integrated Nile drainage network. Geology 28, 343–346.
Tripathy-Lang, A.K., Monteleone, B.D., van Soest, M.C., Hodges, K.V., 2013. Laser (U-Th)/He thermochronology of detrital zircons as a tool for studying surface processes in modern catchments. Journal of Geophysical Research-Earth Surface 118, 1333–1341.
Vezzoli, G., Forno, M.G., Andò, S., Hron, K., Cadoppi, P., Rossello, E., Tranchero, V., 2010. Tracing the drainage change in the Po basin from provenance of Quaternary sediments (Collina di Torino, Italy). Quat. Int. 222, 64–71.
Vezzoli, G., Garzanti, E., Limonta, M., Andò, S., Yang, S., 2016. Erosion patterns in the Changjiang (Yangtze River) catchment revealed by bulk-sample versus single-mineral provenance budgets. Geomorphology 261, 119–177.
Wittke, J.H., Smith, D., Wooden, J.L., 1989. Origin of Sr, Nd and Pb isotopic systematics in high-Sr basalts from central Arizona. Contrib. Mineral. Petrol. 101, 57–68.
Yang, S., Li, C., Yokoyama, K., 2006. Elemental compositions and monazite age patterns of core sediments in the Changjiang Delta: implications for sediment provenance and development history of the Changjiang River. Earth Planet. Sci. Lett. 245, 762–776.
Zhang, Z., Tyrrell, S., Li, C.A., Daly, J.S., Sun, X., Li, Q., 2014. Pb isotope compositions of detrital K-feldspar grains in the upper-middle Yangtze River system: implications for sediment provenance and drainage evolution. Geochem. Geophys. Geosyst. 15, 2765–2779.